

Aus der Abteilung Pädiatrische Hämatologie und Onkologie

Klinik für Kinder- und Jugendmedizin

(Prof. Dr. med. C. Kramm)

der Medizinischen Fakultät der Universität Göttingen

**Complementary medicine treatment
options for children with diffuse intrinsic
pontine gliomas**

INAUGURAL-DISSERTATION

zur Erlangung des Doktorgrades

der Medizinischen Fakultät der

Georg-August-Universität zu Göttingen

vorgelegt von

Bente Pohlmeier

aus

Bremen

Göttingen 2023

Dekan: Prof. Dr. med. W. Brück

Betreuungsausschuss

Betreuer/in Prof. Dr. med. C. Kramm

Ko-Betreuer/in: Prof. Dr. med. E. Heßmann

Prüfungskommission

Referent/in Prof. Dr. med. C. Kramm

Ko-Referent/in: Prof. Dr. med. E. Heßmann

Drittreferent/in: Prof. Dr. T. Meyer

Datum der mündlichen Prüfung: 11.04.2024

Hiermit erkläre ich, die Dissertation mit dem Titel "Complementary medicine treatment options for children with diffuse intrinsic pontine gliomas" eigenständig angefertigt und keine anderen als die von mir angegebenen Quellen und Hilfsmittel verwendet zu haben.

Aachen, den

(Unterschrift)

Index of contents

Index of figures	III
Index of tables.....	III
Abbreviations	IV
1 Introduction	1
1.1 Pediatric high grade glioma.....	1
1.2 Epigenetic and its role in tumorigenesis.....	2
1.3 The epigenetic role of the H3K27M-mutation.....	4
1.4 Therapy of diffuse intrinsic pontine gliomas	5
1.5 Therapeutic effects of Curcumin	6
1.6 Therapeutic effects of Boswellic acids	7
1.7 Aim of this study	9
2 Material and Methods.....	11
2.1 Material.....	11
2.1.1 Cell lines and culture conditions	11
2.1.2 Curcumin, Boswellic acid and temozolomide.....	12
2.1.3 Instruments, consumables and basic chemicals and reagents	13
2.1.4 Buffers and solutions	17
2.1.5 Commercial kits and enzymes	19
2.1.6 Antibodies.....	19
2.1.7 Software	20
2.2 Methods	21
2.2.1 Cell culture.....	21
2.2.2 MTT-cell viability assay	21
2.2.3 Irradiation assay	21
2.2.4 Protein isolation and determination of protein concentration.....	22
2.2.5 SDS-PAGE and western blot analyses	23
2.2.6 Sphere formation assay.....	24
2.2.7 Colony formation assay	24
2.2.8 RNA isolation	25
2.2.9 Library preparation, mRNA sequencing and data analysis	25
2.2.10 Statistical analysis.....	26
3 Results.....	27
3.1 Curcumin	27
3.1.1 Curcumin reduces cell viability in pedHGG cells in a dose dependent manner.....	27
3.1.2 Curcumin sensitizes GBM-001 cells to temozolomide.....	28

3.1.3	Curcumin reduces H3K27- and H4K8-acetylation in DIPG-007, but not in GBM-001 cells	30
3.1.4	Curcumin reduces clonogenicity in DIPG-007 cells and proliferation in pedHGG cells.....	31
3.1.5	Curcumin induces cell cycle arrest and apoptosis in DIPG-007 cells.....	34
3.2	Boswellic acids	38
3.2.1	AKBA reduces cell viability most efficiently in pedHGG cells.....	38
3.2.2	Boswellic acids increase the cell viability reducing effect of temozolomide in pedHGG cells	40
3.2.3	Boswellic acids show no effects on histone modifications in pedHGG cells	42
3.2.4	Boswellic acids reduce clonogenicity in dependence on the phenotype and cell line	43
3.2.5	AKBA has no effect on gene transcription.....	46
4	Discussion.....	47
4.1	The role of Curcumin in diffuse intrinsic pontine glioma	47
4.2	The role of Boswellic acids in diffuse intrinsic pontine glioma	55
4.3	Are Curcumin and Boswellic acids potential complementary treatment options?	59
5	Conclusion	62
6	References	64

Index of figures

Figure 1: Curcumin reduces cell viability in pedHGG cells in a dose dependent manner.	28
Figure 2: Curcumin sensitizes GBM-001 cells to treatment with TMZ.	30
Figure 3: Curcumin reduces H4K8ac and H3K27ac in DIPG-007 cells in a dose dependent manner.	31
Figure 4: Curcumin reduces sphere formation ability and stemness-marker expression in DIPG-007 cells.	33
Figure 5: Curcumin reduces colony formation ability in pedHGG cells.	34
Figure 6: Curcumin influences the cell cycle and induces apoptosis in DIPG-007 cells.	35
Figure 7: Curcumin downregulates genes associated with cell cycle progression and activates genes that are involved in apoptosis in DIPG-007 cells.	36
Figure 8: Curcumin increases Cleaved Caspase 3 levels in DIPG-007 cells.	37
Figure 9: AKBA reduces cell viability in pedHGG cells in a dose dependent manner.	39
Figure 10: BA increase the cell viability reducing effect of TMZ in pedHGG cells.	41
Figure 11: BA have no effect on epigenetic histone modifications.	42
Figure 12: BA reduce colony formation ability in DIPG-007 cells.	44
Figure 13: β -BA induces sphere formation ability in pedHGG cells.	45

Index of tables

Table 2.1 Composition of culture media	11
Table 2.2 Supplements for culture media	12
Table 2.3 Instruments	13
Table 2.4 Consumables	14
Table 2.5 Chemicals and reagents	15
Table 2.6 Composition of buffers and solutions	17
Table 2.7 Commercial kits and enzymes	19
Table 2.8 Primary antibodies	19
Table 2.9 Secondary antibodies	20
Table 2.10 Software	20
Table 2.11 Compositions of stacking and separating SDS-PAGE gels	23

Abbreviations

α -BA	α -Boswellic Acid
AKBA	3-O-Acetyl-11-Keto- β -Boswellic Acid
APS	Ammonium persulfate
β -BA	β -Boswellic Acid
BA	Boswellic acids
BBB	Blood-brain-barrier
BSA	Albumine bovine fraction V
CAM	Complementary and alternative medicine
CBP	Cyclic adenosine monophosphate response element binding protein binding protein
CE buffer	Cytoplasmatic extract buffer
CNS	Central nervous system
CSC	Cancer stem cell
DAVID	Database for Annotation, Visualization and Integrated Discovery
DIPG	Diffuse intrinsic pontine glioma
DMG	Diffuse midline glioma
DMSO	Dimethyl sulfoxide
DMEM	Dulbecco's Modified Eagle's Medium
ECL	Enhanced chemiluminescence
EDTA	Ethylenediaminetetraacetic acid
EGF	Epidermal growth factor
EZH2	Enhancer of Zeste homolog 2
FCS	Fetal calf serum
FDR	False discovery rate
FGF	Fibroblast growth factors
GBM	Glioblastoma
GIC	Glioma initiating cells
GO	Gene ontology
H3K27ac	H3K27-acetylation
H3K27me3	H3K27-trimethylation
H3WT	H3K27-wildtype
H4K8ac	H4K8-acetylation

HAT	Histone acetyl transferase
HEPES	4-(2-hydroxyethyl)-1-piperazineethanesulfonic acid
HRP	Horseradish peroxidase
KEGG	Kyoto Encyclopedia of Genes and Genomes
LPP	Laemmli probe buffer
LT buffer	Separating buffer
LTC	Long-term adult GBM cell lines
MGMT	Methyl guanine methyl transferase
MEM NEAA	Minimum essential medium non-essential amino acids
MTT	3-(4,5-dimethylthiazol-2-yl)-2,5-diphenyltetrazolium bromide
NE buffer	Nuclear extract buffer
NP40	Nonidet-P40
p-gp	P-glycoprotein
PAINS	Pan-assay interference compounds
PBS	Phosphate buffered saline
PDGF	Platelet-derived growth factor
pedHGG	Pediatric high grade glioma
PI3	Phosphoinositid-3
PMSF	Phenylmethylsulfonyl fluoride
PRC2	Polycomb repressive complex 2
PTM	Post translational modification
ROS	Reactive oxygen species
SDS	Sodium dodecyl sulfate
SDS-PAGE	Sodium dodecyl sulfate-polyacrylamide gel electrophoresis
SEM	Standard error of the mean
SIOPE BTG	International Society of Pediatric Oncology Europe Brain Tumor Group
TAE	Tris-acetate-EDTA
TBS-T	TRIS buffered saline with Tween 20
TEMED	N,N,N',N'-Tetramethylethylenediamine
TMZ	Temozolomide
TSM	Tumor stem media
UT buffer	Stacking buffer
WHO	World Health Organization

1 Introduction

1.1 Pediatric high grade glioma

Pediatric cancer of the central nervous system (CNS) represents the second most common cancer in children after leukemia and accounted for 23.6% of all pediatric cancer in 2019 in Germany (Erdmann et al. 2020). One out of 1 400 children under the age of 18 years is diagnosed with a CNS tumor and 20% of the patients die within the first 5 years after their diagnosis (Erdmann et al. 2020).

Tumors of the CNS are graded by the World Health Organization (WHO) from 1 to 4 and are preferentially classified according to histological criteria, most recently also by additional molecular parameters (Ward et al. 2014; Louis et al. 2016; Louis et al. 2021). WHO grade 3 and 4 pediatric tumors of the CNS are called pediatric high grade glioma (pedHGG). Before the revised 4th edition of the WHO classification in 2016 (Louis et al. 2016) in which for the first time molecular parameters were introduced for CNS tumor diagnosis, diffuse pedHGG comprised the same diagnoses as their adult counterparts: anaplastic astrocytoma (WHO grade III), anaplastic oligodendroglioma (WHO grade III), diffuse intrinsic pontine glioma (DIPG) (WHO grade IV), glioblastoma (GBM) (WHO grade III), giant cell glioblastoma (WHO grade III), and gliosarcoma (WHO grade III) (Filbin and Suva 2016). In 2016, DIPG were resolved within the new CNS tumor entity of diffuse midline glioma, H3K27M (WHO grade IV) which were defined by the H3K27M mutation, midline location (mostly involving thalamus/basal ganglia, brainstem, and spinal structures) as well as a diffuse growth pattern (Louis et al. 2016). With the publication of the completely new 5th edition of the WHO classification in 2021, the traditional diagnoses of glioblastoma and anaplastic astrocytomas completely vanished for pedHGG and completely new tumor entities were introduced, mostly now defined by molecular parameters and arabic letters to describe the now called CNS grade of the expected clinical phenotype (Louis et al. 2021):

- Diffuse midline glioma, H3 K27-altered (grade 4)
- Diffuse hemispheric glioma, H3 G34-mutant (grade 4)
- Diffuse pediatric type high-grade glioma, H3-wildtype and IDH-wildtype (grade 4)
- Infant-type hemispheric glioma (no CNS grade).

All the “old” pedHGG diagnoses are now distributed among the four new diagnoses with DIPG exclusively found among diffuse midline gliomas (DMG).

All pedHGG only represent about 8 to 12% of all pediatric tumors of the CNS, they have a dismal prognosis (Fangusaro 2012). Most pedHGG arise in the pons (DIPG) and in the cerebral hemispheres (Filbin and Suva 2016). The median survival for patients with DIPG is eleven months, less than 10% survive the first two years after diagnosis, and 2% are longtime survivors (survival longer than five years after diagnosis) (Hoffman et al. 2018). Thereby, patients with DIPG/DMG display the worst prognosis of all patients with pedHGG (Mackay et al. 2017).

Today, many DIPG are still diagnosed through clinical appearance and magnetic resonance imaging as it was done for many years (Ballester et al. 2013) although the new WHO diagnosis cannot be made without a biopsy to detect the H3K27 alteration within the tumor cells. Biopsies still do not improve the diagnosis of the DIPG, alter the standard treatment approach, nor survival outcome, but may be accompanied by an increased postsurgical morbidity. Thus, biopsied should ideally only be performed in DIPG for research purposes (Ballester et al. 2013). Nevertheless, by avoiding biopsies in general as it had happened for nearly 20 years the genetic insight into DIPG tumors and its impact on tumor biology has been limited and delayed (van Veldhuijzen Zanten et al. 2017).

While a substantial part of adult high grade glioma develop through multiple mutations of low grade tumors, most DIPG are primary brain tumors and are therefore usually diagnosed in the primary setting (Braunstein et al. 2017). Consequently, DIPG carry a lower mutation burden than their adult counterparts with a median of two non-silent and 15 coding mutations (Filbin and Suva 2016).

In 2012, a mutation highly specific for DIPG and thalamic and spinal pedHGG was discovered in the histone genes *H3F3A* encoding histone H3.3 or *HIST1H3A/B/C* encoding histone H3.1 leading to the substitution of lysine 27 to methionine (Schwartzentruber et al. 2012; Gerges et al. 2013). The H3K27M-mutation was observed to influence the epigenetic landscape and defined the new entity of DMG in the most recent WHO classification as already pointed out above (Bender et al. 2013; Lewis et al. 2013; Louis et al. 2021).

1.2 Epigenetic and its role in tumorigenesis

The term “epigenetic” can be defined as “the structural adaptation of chromosomal regions so as to register, signal or perpetuate altered activity states” (Bird 2007) and includes different

mechanisms such as DNA methylation, noncoding RNA and histone modification (Li and Tollefsbol 2016). Since the H3K27M-mutation leads to changes in histone modifications (Lewis et al. 2013), the focus of this thesis is on histone modifications as epigenetic regulators.

The DNA in eucaryotic cells is wrapped around a histone octamer containing two copies of each of the four core histones H2A, H2B, H3 and H4, called the nucleosome. The binding of the linker histone H1 influences the compaction of the chromatin (Ramakrishnan 1997). Due to the negative charge of the DNA, the positively charged amino acids lysine and arginine in the N-terminal tail of the histones interact with the DNA, which leads to different states of condensation (Korolev et al. 2018). Depending on its transcriptional activity, the chromatin can dynamically change between the highly condensed heterochromatin or the decondensed euchromatin. Heterochromatin is transcriptionally inactive while euchromatin is transcriptionally active. Post-translational modifications (PTM) of the N-terminal tail of histones play an important role in modulation of condensation of chromatin and the recruitment of non-histone proteins. Thus, PTM regulate gene activation and repression without affecting the DNA sequence (Zhang et al. 2014; Kouzarides 2007). There are different types of PTM: Acetylation, methylation, phosphorylation, ubiquitylation, sumoylation, ADP ribosylation, deamination, and proline isomerization (Kouzarides 2007).

Adding and removing of histone PTM is a dynamic process carried out by different enzymes often termed as “writers” and “erasers”. These modifications are added to distinct amino acid residues throughout the histone, offering the possibility to regulate both gene activation and gene repression (Cohen et al. 2011). The effect of PTM depends on their direct influence on histones and on their location within the tail of the histone. While acetylation of lysine removes its positive charge, thus leading to relaxation of chromatin and gene activation, methylation of histones can be associated with either gene activation (H3K4, 36 and 79) or gene repression (H3K9 and 27 and H4K20) depending on its location on the histone tail (Sadakierska-Chudy and Filip 2015). Different PTM added to the same amino acid on histone tails can lead to an opposed transcriptional state. For example: H3K27-acetylation (H3K27ac) leads to gene activation while H3K27-trimethylation (H3K27me3) leads to gene repression (Zhang et al. 2015). Consequently, acetylation and methylation of lysine are mutually exclusive (Kouzarides 2007).

In addition to directly influencing gene expression, PTM influence the addition or removal of other neighboring PTM (Sadakierska-Chudy and Filip 2015). For instance: H3K27me3 stimulates the addition of H3K27me3 on neighboring nucleosomes (Cohen et al. 2011).

The pattern of PTM determines different processes in cells such as differentiation, development and pluripotency, hence playing an important role in development of cancer and other diseases (Cohen et al. 2011).

1.3 The epigenetic role of the H3K27M-mutation

Since the PTM methylation and acetylation typically occur on the amino acid lysine, the H3K27M-mutation (lysine 27 is switched to methionine) has an impact on PTM (Griffith and Holmes 2019). Lysine 27 is located at the N-terminal tail of histone 3 where PTM take place (Schwartzentruber et al. 2012). It was observed that H3K27M-mutated cells express a global reduction and a local gain of H3K27me3 and globally increased levels of H3K27ac (Lewis et al. 2013; Bender et al. 2013). Since H3K27me3 is associated with gene silencing, its decreased level leads to reduction of its gene silencing effect, whereas the increased level of H3K27ac, leads to activation of gene transcription (Filbin and Suva 2016).

The underlying mechanisms of the changes in the epigenetic landscape in H3K27M-mutant cells are not fully understood yet. Under physiological conditions, the lysine acetyltransferases cyclic adenosine monophosphate response element binding protein binding protein (CBP) and p300, a multitarget acetyltransferases, introduce the H3K27ac (Jin et al. 2011). The H3K27me3 is introduced by the histone methyltransferase Enhancer of Zeste homolog 2 (EZH2), the enzymatic subunit of the polycomb repressive complex 2 (PRC2) (Margueron and Reinberg 2011). In H3K27M-mutated cells, only 3 to 17% of H3 are mutated. Still, a global loss of H3K27me3 was observed in these cells, suggesting that the mutation has a dominant negative effect, which is hypothesized to occur through inhibition of PRC2 by the H3K27M-mutation (Filbin and Suva 2016).

The effect of the H3K27M-mutation could be observed in cultured cells. When compared to H3K27-WT cells, H3K27M-mutated cells express higher proliferation, stem cell-like characteristics and are more resistant towards irradiation (Wiese et al. 2020). Furthermore, it was observed that the inhibition of demethylation of H3K27 and thereby partial restoration of its methylation led to an anti-tumor effect (Filbin and Suva 2016). These findings suggest that the H3K27M-mutation influences tumorigenesis and possible therapy options, which is relevant for potential treatment options since more than 85% of DIPG carry an H3K27M-mutation (Castel et al. 2018).

1.4 Therapy of diffuse intrinsic pontine gliomas

Currently, DIPG are not curable and there are no international guidelines for treatment in Europe (El-Khouly et al. 2019). Therefore, the treatment of DIPG is similar to those of their adult counterparts: it consists of resection of the tumor, if possible, in combination with irradiation and chemotherapy. However, the location of the tumor within the pons displays an obstacle for resection since it is difficult to access and proximate to vital brain centers (Filbin and Suva 2016). In addition, DIPG are only partially sensitive to irradiation (Filbin and Suva 2016). Since there are no international guidelines for treatment, different chemotherapeutics are used to treat DIPG. However, the most frequently used chemotherapeutic for children with DIPG is temozolomide (TMZ) (El-Khouly et al. 2019), an alkylating agent which adds a methyl group to purine and pyrimidine in the DNA and therefore leads to DNA damage and apoptosis (Karachi et al. 2018).

In summary, the therapy of DIPG represents a big challenge because of the rarely performed resection and a strong resistance towards radio- and chemotherapy (Filbin and Suva 2016). Moreover, there has been no significant improvement of therapy in the last 50 years (Castel et al. 2015).

Since the survival rates are very low and therapeutic options are limited, parents of patients with DIPG often resort to complementary and alternative medicine (CAM). An online survey executed in 2020 by the International Society of Pediatric Oncology Europe Brain Tumor Group (SIOPE BTG) investigated the application of CAM in DIPG patients. Participants of the study included parents and caregivers of affected children (n=120), which were recruited via parent foundations or their physician, and healthcare professionals (n=75), recruited via the electronic mailing list of the SIOPE BTG. It was shown that 69% of the participants of the survey used some form of CAM to treat the affected child. In case of parental relationship, the CAM application was always intended to actively treat the tumor. Less than 10% viewed CAM as an alternative to conventional treatment, while over 90% used CAM in combination with conventional treatments, often without the knowledge of the treating physicians. Moreover, patients with diagnosis after 2016 were more likely to receive any form of CAM than those diagnosed before 2016. Amongst the five most frequently used CAM were Curcumin and Boswellic acids (BA) (El-Khouly et al. 2021). Both agents harbor various properties which qualify them as potential complementary treatment options for children with pedHGG.

1.5 Therapeutic effects of Curcumin

Curcumin is extracted from the rhizomes of *Curcuma longa* and is mostly known as an Indian spice which is essential for the curry powder's yellow color. However, Curcumin represents an important reactive agent in traditional Indian and Chinese medicine and has been used for medical purposes for many years, the first reports of medical use of Curcumin are recorded in 1748. Its medical use had been limited to eastern countries due to the development of western medicine. The first article about its use in human disease was published in 1937, awakening the interest in the use of Curcumin for medical purposes (Gupta et al. 2013; Kumar et al. 2015; Oppenheimer 1937). Today over 13 000 scientific articles have been published, investigating the effect of Curcumin (Kumar et al. 2015). It is suggested that Curcumin exhibits various health benefitting properties such as anti-inflammatory, anti-oxidant and anti-mutagenic effects (Pulido-Moran et al. 2016). The anti-cancer effect of Curcumin were first reported in the 1980's and have since been observed in various cancers amongst others in adult glioblastoma (Gersey et al. 2017; Hesari et al. 2018; Shin et al. 2019; Kuttan et al. 1985; Shanmugam et al. 2015).

Therefore, Curcumin was observed to exhibit many properties which could be relevant for its potential to treat pedHGG which are listed in the following paragraphs.

Curcumin (diferuloyolmethane) is a hydrophobic polyphenol and was observed to pass the blood-brain-barrier (BBB) independently of the p-glykoprotein (p-gp) (Kumar et al. 2015; Perry et al. 2010). The p-gp can actively discard material from the brain into the circulatory system and therefore plays an important role for the multi-drug resistance (Mesev et al. 2017). The p-gp independence of Curcumin and its ability to pass the BBB are important for its use as treatment for brain tumors such as pedHGG since it needs to be able to reach the tumor site. However, it was also reported that bioavailability after oral administration of Curcumin in healthy patients is very limited due to its poor absorption in the small intestines and its fast metabolism in the liver (Dei Cas and Ghidoni 2019).

Treatment using Curcumin resulted in dose dependent reduction of cell viability in adult GBM cells *in vitro*. Furthermore, treatment of adult GBM cells with Curcumin led to a reduction of proliferation and decreased ability to form colonies and spheres (Gersey et al. 2017). The examination of the effect of Curcumin on the cell cycle showed that Curcumin inhibits proliferation through induction of cell cycle arrest in various cell lines (Xu et al. 2018). In addition, Curcumin induced apoptosis, thus reducing the viability of colon carcinoma and head and neck squamosa carcinoma cells by activating Caspase 3 (Xi et al. 2015; Montgomery et al. 2016).

The treatment for DIPG consists of treatment with TMZ combined with irradiation (El-Khouly et al. 2019). In combination with radiotherapy, Curcumin was observed to sensitize adult glioblastoma cells to irradiation (Dhandapani et al. 2007). Furthermore, Curcumin was observed to sensitize adult glioblastoma cells to TMZ (Dhandapani et al. 2007; Yin et al. 2014).

Various studies have investigated the epigenetic impact of Curcumin. Curcumin was observed to inhibit the histone-acetyltransferase-activity of CBP, reducing the acetylation of histone 3 and 4 induced by CBP (Balasubramanyam et al. 2004; Lu et al. 2014). Furthermore, Yan et al. (2017) investigated the effect of Curcumin on histone hyperacetylation induced by alcohol in fetal cardiac progenitor cells of mice. Treatment with Curcumin resulted in a decrease of the induced hyperacetylation.

On the other hand, Curcumin was also observed to reduce the expression of EZH2 in pancreatic ductal adenocarcinoma cells and in lung cancer cells (Yoshida et al. 2017; Wu et al. 2016). EZH2 is a subunit of the PRC2 complex and introduces the H3K27me3 (Margueron and Reinberg 2011). Therefore, a reduced expression of EZH2 might influence the epigenetic landscape.

Dose-escalating studies in humans showed that the tolerance for Curcumin at oral doses up to 12 000 mg per day is excellent. The study did not define a maximum tolerated dose (Lao et al. 2006).

However, data for treatment with Curcumin in pedHGG and DIPG cells is limited. Samarth et al. (2018) reported that Curcumin induced significant cell death in a 2D tissue culture of DIPG cells at concentration of 37.5 μ M. Furthermore, Curcumin enhanced cell death in DIPG cells after delivery of tumor necrosis factor- α transgene by targeted-bacteriophage vector (Samarth et al. 2018).

1.6 Therapeutic effects of Boswellic acids

The source of BA is the gum resin of *Boswellia* species, trees of family Burseraceae which are native in India, Northern Africa, and the Middle East. The main source of the gum resin is *Boswellia serrata* and *Boswellia carteri* but it is more commonly known as Indian frankincense, Salai Guggal or Indian olibanum. It has been used for religious purposes and in Ayurvedic medicine for centuries (Ahmed et al. 2015; Beghelli et al. 2017; Roy et al. 2019). The gum resin contains different types of BA, which are considered the most bioactive constituents of the gum resin (Mannino et al. 2016; Du et al. 2015; Roy et al. 2019), of which the three α -

Boswellic acid (α -BA), β -Boswellic acid (β -BA), and 3-O-acetyl-11-keto- β -Boswellic acid (AKBA) were used in this study.

BA are highly lipophilic, pentacyclic triterpenes and mostly known for their anti-inflammatory properties. However, they are multitargeting compounds and are able to modulate the pathogenesis of different diseases through influencing several pathways (Roy et al. 2019). Various articles suggest that BA exhibits anti-inflammatory, anti-bacterial, anti-fungal, anti-cancer, neuroprotective, and analgetic activities (Prabhavathi et al. 2014; Mannino et al. 2016). Some properties which could be important for their use as therapeutic agents against pedHGG are listed in the following paragraphs.

BA need to cross the BBB to reach the tumor site. An *in vivo* experiment in rats investigated the ability of BA to cross the BBB. Amongst others α -BA, β -BA and AKBA were investigated and all three BA were confirmed in the rat's brain eight hours after oral administration, concluding that BA can cross the BBB (Gerbeth et al. 2013).

Furthermore, the effect of BA on the cell viability of different cancer cells has been investigated. For instance, frankincense oil was observed to reduce cell viability of bladder cancer cells *in vitro* (Frank et al. 2009) and BA reduced cell viability and induced apoptosis in colon cancer cells *in vitro* (Wang et al. 2018). BA also reduced cell viability of adult glioblastoma cells *in vitro* and decreased their clonogenic ability (Schneider and Weller 2016; Conti et al. 2018).

The therapy of DIPG very often consists of a combination of TMZ with irradiation (El-Khouly et al. 2019). A study investigating the effect of BA in adult glioblastoma cells combined with either TMZ or irradiation suggests that the effect was mostly additive and never antagonistic (Schneider and Weller 2016). Another *in vivo* study on adult glioblastoma in female athymic CD-1 nude mice reported an increased inhibition of tumor growth after treatment with AKBA in combination with irradiation when compared to irradiation alone (Conti et al. 2018).

Furthermore, BA were reported to influence the epigenetic landscape in colorectal cancer cells *in vitro*. Treatment with AKBA induced genome wide DNA demethylation and inhibited DNA methyltransferase activity and re-activated a subset of tumor suppressor genes (Shen et al. 2012).

The use of BA supplements for medical conditions has already been investigated in the clinical setting. For example, phase II studies used orally applied BA supplements as treatment for

osteoarthritis or cerebral edema after irradiation and reported no severe adverse effects (Kirste et al. 2011; Sengupta et al. 2008).

However, no study has investigated the effects of BA in pedHGG.

1.7 Aim of this study

Since treatment for DIPG patients has not yet improved the poor prognosis, there is a need for new therapeutic strategies. Both Curcumin and BA harbor many properties which qualify them as potential alternative or at least supplementary therapeutic options for DIPG patients. Even though both compounds are already used as therapeutic supplements, the data examining the effect of Curcumin and BA in pedHGG cells is very limited.

Thus, the aim of this study was to investigate the effect of Curcumin and BA *in vitro* in a DIPG cell line and as a control in a pediatric GBM cell line to assess the therapeutic potential of these natural compounds for patients with DIPG and GBM. As the H3K27M mutation is very common in DIPG, the DIPG cell line used in this study is H3K27M-mutated while the control pediatric GBM cell line is H3K27-wildtype (H3WT). The cell lines with different H3-mutation status were used to evaluate if Curcumin and BA exert H3K27M-dependent effects.

Furthermore, to represent the heterogeneity of pedHGG tumors, two distinct cellular phenotypes were used in this study: Gliomaspheres which exhibit a more cancer stem cell (CSC)-like phenotype and more differentiated pedHGG cells grown as adherent monolayer cultures.

Since both Curcumin and BA were able to influence cell viability and clonogenicity in different cancer cells amongst others in adult glioblastoma (Frank et al. 2009; Schneider and Weller 2016; Gersey et al. 2017), the impact of Curcumin and BA on cell viability and clonogenicity in pedHGG cells were investigated.

Previous studies have shown that Curcumin and BA influence the impact of the most commonly used treatment for pedHGG patients consisting of radiation in combination with chemotherapeutic TMZ in other cancers (Dhandapani et al. 2007; Yin et al. 2014; Schneider and Weller 2016; Conti et al. 2018; El-Khouly et al. 2019). Therefore, the influence of Curcumin and BA combined with standard treatment in pedHGG cells was investigated.

The epigenetic alterations induced by the H3K27M-mutation play an important role in tumorigenesis (Castel et al. 2018). In addition, both Curcumin and BA have been reported to influence the epigenetic landscape (Shen et al. 2012; Yan et al. 2017; Balasubramanyam et al.

2004). Thus, the impact of Curcumin and BA on important genetic alterations such as H3K27ac and H3K27me3 was examined in pedHGG cells.

Since epigenetic changes influence the transcription, the transcriptome of DIPG cells after treatment with Curcumin and BA was also analyzed to investigate the effect of Curcumin and BA on gene expression and potential signal transduction pathways.

2 Material and Methods

2.1 Material

2.1.1 Cell lines and culture conditions

Two different cell lines were used in this study: H3.3K27M-mutated HSJD-DIPG-007 cells referred to as DIPG-007 cells and H3-wildtype HSJD-GBM-001 cells referred to as GBM-001 cells. In the following, both cell lines together are referred to as pedHGG cells. Human derived DIPG-007 and human derived GBM-001 cells were kindly supplied by Angel Montero Carcaboso (Hospital Sant Joan de Déu, Barcelona, Spain).

Cells were cultured in tumor stem media (TSM work) under spheroid conditions or as adherent monolayer cells in TSM diff. The composition of the different cell culture media is listed in Table 2.1.

Table 2.1 Composition of culture media

Medium	Composition
TSM base	1:1 Neurobasal [®] -A Medium: DMEM/F-12, 1% HEPES buffer, 1mM Sodium pyruvate, 1x MEM NEAA, 1x GlutaMAX [™] -I
TSM diff	TSM base, 10% FCS
TSM work	TSM base, 1x B27 [®] Supplement, 20 ng/ml EGF, 20 ng/ml FGF, 10 ng/ml PDGF-AA, 10 ng/ml PDGF-BB, 2 µg/ml Heparin

The supplements for culture media and their manufacturer can be found in Table 2.2.

Table 2.2 Supplements for culture media

Additional supplement	Manufacturer
B27 [®] Supplement (50x)	Gibco [®] by life technologies [™]
DMEM/F-12 (1:1) (1x)	Gibco [®] by life technologies [™]
Fetal Calf Serum (FCS)	Biochrom
GlutaMAX (100x)	Gibco [®] by life technologies [™]
Heparin sodium salt from porcine intestinal mucosa	Sigma-Aldrich
HEPES (4-(2-hydroxyethyl)-1-piperazine-ethanesulfonic acid) Buffer	Gibco [®] by life technologies [™]
MEM NEAA (100x) (minimum essential medium non-essential ammino acids)	Gibco [®] by life technologies [™]
Neurobasal [®] -A Medium	Gibco [®] by life technologies [™]
OptiMEM [®] I	Gibco [®] by life technologies [™]
PDGF-AA	PeproTech
PDGF-BB	PeproTech
Penicillin-Streptomycin	Gibco [®] by life technologies [™]
Recombinant human EGF (epithelial growth factor)	PeproTech
Recombinant human FGF (fibroblast growth factors)	PeproTech
Sodium-Pyruvate 100mM (100x)	Gibco [®] by life technologies [™]

2.1.2 Curcumin, Boswellic acid and temozolomide

Curcumin (Diferuloylmethane) powder was obtained from Selleckchem (Munich, Germany) and dissolved in dimethyl sulfoxide (DMSO). AKBA powder, α -BA powder, and β -BA powder were obtained from Extrasynthese (Genay Cedex, France) and dissolved in DMSO. In the following, all three compounds AKBA, α -BA and β -BA are referred together as BA. TMZ

powder was supplied by Selleckchem (Munich, Germany) and dissolved in DMSO. Aliquots of TMZ, Curcumin, and BA were stored at -80°C .

2.1.3 Instruments, consumables and basic chemicals and reagents

The instruments used in this study were obtained from the manufacturers listed in Table 2.3.

Table 2.3 Instruments

Instrument	Manufacturer
BioDocAnalyzer	Biometra, Göttingen, Germany
Blotting system	Biometra, Göttingen, Germany
Centrifuge 5415D	Eppendorf, Hamburg, Germany
Centrifuge 5810R	Eppendorf, Hamburg, Germany
Electrophoresis power supply	BioRad, Feldkirchen, Germany
Electrophoresis system for agarose gels	BioRad, Feldkirchen, Germany
HiSeq4000	Illumina, Munich, Germany
Incubator BBD6220	Thermo Scientific, Braunschweig, Germany
Infinite F50 absorbance plate reader	Tecan Group Ltd., Männedorf, Switzerland
Luminescent image analyzer LAS-4000 mini	Fujifilm, Düsseldorf, Germany
Mini-PROTEAN Tetra cell electrophoresis system	BioRad, Feldkirchen, Germany
Micropipett (2.5 μl , 10 μl , 100 μl , 200 μl , 1000 μl)	Eppendorf, Hamburg, Germany
Multipipett	Eppendorf, Hamburg, Germany
Neubauer cell counting chamber	Brand, Wertheim, Germany
RS 225 X-Ray Research System	Gulmay Medical Systems, Surrey, Camberley, UK

Instrument	Manufacturer
Sonifier UP50H	Hielscher Ultrasonics GmbH, Teltow, Germany
Spectrophotometer NanoDrop® ND-1000	Thermo Scientific, Braunschweig, Germany
SynergyMx microplate reader	BioTek®, Bad Friedrichshall, Germany
Thermomixer 5436	Eppendorf, Hamburg, Germany
Vortex VF2	IKA, Staufen, Germany

The consumables used in this study are displayed in Table 2.4.

Table 2.4 Consumables

Consumables	Manufacturer
Cell scraper	Sarstedt
Combitips	Eppendorf
Dish100, Cell+ (10 cm)	Sarstedt
Falcon tubes (15 ml)	Sarstedt
Falcon tubes (50 ml)	Greiner bio-one
Flasks for cell culture (T75 and T175)	Sarstedt
Immobilon-P PVDF membrane (pore size 0.45 µm)	Merck
Nuclon Delta Surface cell culture plates (6-well, 12-well and 96-well)	Thermo Scientific
Pasteur pipettes	Brand
Pipette filter tips (10 µl, 100 µl, 200 µl, 1000 µl)	Starlab
Pipette tips (10 µl, 200 µl, 1000 µl)	Sarstedt
Reaction tubes (1.5 ml and 2 ml)	Sarstedt

Consumables	Manufacturer
Serological pipettes (5 ml, 10 ml, 25 ml)	Sarstedt
Whatman filter paper	Sartorius

The basic chemicals and reagents used in this study are presented in Table 2.5.

Table 2.5 Chemicals and reagents

Chemical/reagent	Manufacturer
6 X DNA loading dye	Thermo Scientific
β -Mercaptoethanol	Sigma-Aldrich
Acetic acid	Merck
Acetic acid glacial	Merck
AgaPure™ Agarose LE	Canvax
Albumin bovine Fraction V, protease-free (BSA)	Serva
Albumin Standard	Thermo Scientific
Ammonium persulfate (APS)	Roth
BC Assay reagent A	Interchim
BC Assay reagent B	Interchim
BlueStar prestained protein marker	Genetics
Bromphenole blue	Sigma-Aldrich
Coomassie Brilliant Blue	BioRad
Crystal Violet solution	Sigma-Aldrich
Dimethyl sulfoxide (DMSO)	Roth
Dithiothreitol	AppliChem
Ethanol	Roth
Ethidium bromide	Roth

Chemical/reagent	Manufacturer
Ethylenediaminetetraacetic acid (EDTA)	Sigma-Aldrich
Formaldehyde solution min. 37%	Merck
Formic acid 98-100%	AppliChem
Glycerin	Merck
Glycerol	Fisher Chemicals
Glycin	Roth
Glycoblue	ThermoScientific
Isopropanol	Roth
Luminol	Sigma-Aldrich
Magnesium chloride (MgCl)	Roth
Methanol	Chemsolute
N,N,N',N'-Tetramethylethylenediamine (TEMED)	Roth
Nonidet-P40 (NP40)	Fluka
p-coumaric acid	Sigma-Aldrich
Peroxygen (H ₂ O ₂)	Merck
Phenylmethylsulfonyl fluoride (PMSF)	Serva
Potassium Chloride (KCl)	Roth
Potassium dihydrogen phosphate (KH ₂ PO ₄)	Roth
Powdered milk	Roth
Protease Inhibitor Cocktail Tablets	Roche
Quick-Load Purple 1kb DNA Ladder	New England Bio Labs
Roti®-Phenol/Chloroform/Isoamyl alcohol	Roth
Roti®-Stock 20% SDS	Roth

Chemical/reagent	Manufacturer
Rotiphorese® Gel 40 (1:29)	Roth
Sodium acetate	Roth
Sodium chloride (NaCl)	Roth
Sodium dodecyl sulfate (SDS), ultra-pure	Roth
Di-Sodium hydrogen phosphate (Na ₂ HPO ₄)	Roth
Thiazolyl Blue tetrazolium bromide (MTT)	Alfa Aesar
Tris	Roth
Trypan Blue stain (0.4%)	Gibco® by life technologies™
TrypLE™Express	Thermo Scientific
Tween 20	Sigma-Aldrich

2.1.4 Buffers and solutions

The composition of the buffers and solutions used in the present study are listed in Table 2.6.

Table 2.6 Composition of buffers and solutions

Name	Composition
2x Crystal Violet staining solution	9.6% Crystal Violet solution, 19.2% Formaldehyde (min. 37%), 19.2% Methanol, 19.2% PBS
4x Laemmli probe buffer (LPP)	240 mM Tris-HCl (pH6.8), 40% glycerin, 8% SDS, 20% β-mercaptoethanol, 0.04% bromphenolblue
4x separating (LT) buffer (pH 8.8)	1.5 M Tris-HCl (pH 8.8), 0.4% SDS
4x stacking (UT) buffer (pH 6.8)	0.5 M Tris-HCl (pH 6.8), 0.4% SDS
50x Tris-acetate-EDTA (TAE) buffer	0.571% acetic acid glacial, 0.05 M EDTA, 2 M Tris-HCl (pH 8.0)

Name	Composition
Blocking solution	5% powdered milk/BSA in TBS-T
Blotting buffer	25 mM Tris, 192 mM glycine, 10% methanol
Coomassie destaining solution	10% acetic acid glacial, 20% isopropanol, 70% H ₂ O
Coomassie staining solution	0.2% Coomassie Brilliant Blue, 33% isopropanol, 10% acetic acid
Cytoplasmic Extract (CE) buffer (pH 7.6)	10 mM HEPES buffer, 60 mM KCL, 1 mM EDTA, 0.075% NP40, 1 mM DTT, 1mM PMSF
Enhanced chemiluminescence (ECL) solution A	2.5 mM luminol, 0.36 mM p-coumaric acid, 0.1 M Tris-HCl (pH 8.5)
ECL solution B	0.0182% H ₂ O ₂ , 0.1 M Tris-HCl (pH 8.5)
Laemmli running buffer	25 mM Tris, 192 mM glycine, 0.01% SDS
MTT solution	5 mg/ml MTT in PBS
MTT solvent solution	33% DMSO, 5% formic acid, 62% isopropanol
Nuclear Extract (NE) buffer (pH 8.0)	20 mM Tris Cl, 420 mM NaCl, 1.5 mM MgCl ₂ , 0.2 mM EDTA, 1 mM PMSF, 25% glycerol
Phosphate buffered saline (PBS)	5.48 mM NaCl, 0.108 mM KCl, 0.08 mM KH ₂ PO ₄ , 0.4 mM Na ₂ HPO ₄
TRIS buffered saline with Tween 20 (TBS-T) (pH 7.4)	20 mM Tris-HCl, 150 mM NaCl, 0.1% Tween 20

2.1.5 Commercial kits and enzymes

The commercial kits and enzymes were obtained from the manufacturers listed in Table 2.7.

Table 2.7 Commercial kits and enzymes

Kit	REF number	Manufacturer
GoScript™ Reverse Transcription Mix	A2800	Promega, Walldorf, Germany
TruSeq RNA Library Prep Kit v2	RS-122-2001 RS-122-2002	Illumina, Munich, Germany
SignalFire™ Elite ECL reagent	12757S	Cell Signaling Technology, Danvers, USA
ReliaPrep™ RNA Clean-Up and Concentration System	Z1071	Promega, Walldorf, Germany
ReliaPrep™ RNA Miniprep System	Z6012	Promega, Walldorf, Germany

2.1.6 Antibodies

The primary antibodies and their origin, dilution and distributing company are displayed in Table 2.8.

Table 2.8 Primary antibodies

Primary antibody	Origin	Dilution	REF number	Company
β-actin	mouse	1:5000	A3854	Sigma-Aldrich
Acetyl-Histone H4 (Lys 8)	rabbit	1:1000	2594	Cell Signaling Technology
Caspase 3	rabbit	1:1000	ab90437	abcam
Cleaved Caspase 3	rabbit	1:1000	9541S	Cell Signaling Technology
Histone H3K27ac (Acetyl	rabbit	1:1000	GTX128944	GeneTex

Primary antibody	Origin	Dilution	REF number	Company
Lys27)				
Oct ³ / ₄	mouse	1:1000	61102	Becton Dickinson
Tri-Methyl-Histone (Lys 27) (C36B11)	H3 rabbit	1:1000	9733	Cell Signaling Technology

The matching secondary antibodies, their dilution and distributing company are listed in Table 2.9.

Table 2.9 Secondary antibodies

Secondary antibody	Dilution	REF number	Company
Anti-mouse IgG, horseradish peroxidase (HRP)-linked	1:5000	115-035-174	Dianova
Anti-rabbit IgG, HRP-linked	1:5000	211-032-171	Jackson ImmunoResearch

2.1.7 Software

The software used in this study is displayed in Table 2.10.

Table 2.10 Software

Software	Company
ImageJ. 1.48	National Institute of Health
Magellan for F50 7.0SignalFire™ Elite	Tecan Group Ltd.
Microsoft Office 2013	Microsoft

2.2 Methods

2.2.1 Cell culture

DIPG-007 and GBM-001 cells were cultured in tissue culture flasks in TSM work medium (Table 2.1) and maintained in a saturated incubator at 37°C and 5% CO₂. For seeding and passaging, spheres were collected in 50 ml tubes and centrifuged at 1 000 rpm for 5 min. The supernatant was removed, and spheres were separated enzymatically by trypsin treatment (TrypLE™Express) in combination with gently pipetting up and down. Cells were washed with phosphate buffered saline (PBS) and centrifuged at 1 000 rpm for 5 min. The supernatant was removed, and cells were suspended in 5 ml medium. For cell counting, 100 µl of cell suspension were transferred into 1.5 ml reaction tube and 300 µl Trypan blue was added. The solution was transferred into the Neubauer cell counting chamber (Brand) and cells were counted. Calculated cells were suspended in TSM work for spheroid cell culture or TSM diff for adherent monolayer culture (Table 2.1).

2.2.2 MTT-cell viability assay

To determine the viability of cells after treatment with Curcumin and BA, 3-(4,5-dimethylthiazol-2-yl)-2,5-diphenyltetrazolium bromide (MTT-) cell viability assays were conducted. DIPG-007 and GBM-001 cells were seeded into 96-well-plates at a concentration of 50 000 cells/ml in 50 µl TSM work (Table 2.1) for spheroid or TSM diff (Table 2.1) for adherent monolayer conditions. After incubation for 24 h, cells were treated with 50 µl medium containing the corresponding amounts of Curcumin, BA, or DMSO control. After 72 h, cells were treated with 15 µl MTT solution (5 mg/ml) and incubated for 4 h. To evaluate concentration of formazan, the supernatant was transferred into 1.5 ml reaction tubes. The tubes were centrifuged at maximum speed for at least 10 min. Supernatant was removed and 100 µl MTT solvent solution (Table 2.6) was added to the reaction tubes. The content was transferred back into the plates. The absorbance rate at 560 nm was measured using Tecan's Infinite F50 absorbance plate reader (Tecan Group Ltd.).

2.2.3 Irradiation assay

To determine the effect of Curcumin and BA on standard treatment options for pedHGG consisting of irradiation and TMZ, irradiation assays were performed. For the irradiation assay, 25 000 cells/ml in 50 µl were seeded into 96-well-plates using TSM work medium (Table 2.1). After incubation for 48 h at 37°C, cells were treated with 50 µl Curcumin or BA

alone or in combination with TMZ and incubated for another 24 h at 37°C. The plates received a single irradiation dose of 8 Gy or remained not irradiated for control. Radiation treatment at a dose rate of 1 Gy/min (8 Gy for 8 min) was delivered by a RS 225 X-Ray Research System (Gulmay Medical Systems, Xstrahl Ltd) operated at 200 kV, 15 mA and with 0.5 mm Cu filtration. After another 24 h of incubation at 37°C, cells were treated a second time with Curcumin or BA alone or Curcumin or BA in combination with TMZ and incubated for 72 h. Fifteen µl MTT solution (5 mg/ml) were added to each well. After 4 h of incubation, the content of the wells was transferred into 1.5 ml tubes and centrifuged at maximum speed for 10 min. Supernatant was removed, and 100 µl MTT-solvent-solution was added to the tubes. Resolved cells were transferred back to a 96-well plate, and photometric absorbance was measured at 560 nm using Tecan's Infinite F50 absorbance plate reader (Tecan Group Ltd.).

2.2.4 Protein isolation and determination of protein concentration

For protein isolation, DIPG-007 and GBM-001 cells were seeded at a concentration of 50 000 cells/ml into 10 cm petri dishes with 10 ml TSM work medium (Table 2.1). After incubation for 24 h at 37°C, cells were treated with the indicated concentrations of Curcumin or BA and incubated for 72 h at 37°C. Cells were transferred into 15 ml falcon tubes and centrifuged at 1 000 rpm for 5 min. The supernatant was discarded. Pellets were resuspended in up to 200 µl cytoplasmic extract (CE) buffer (Table 2.6) depending on the pellet size, supplemented with 1x Protease inhibitor Cocktail (Roche) and incubated on ice for 3 min to destroy the cellular membrane and separate the nuclei from the cellular fraction. Preparations were centrifuged at 1 500 rpm at 4°C for 4 min and the supernatant containing the cellular protein was transferred into clean tubes. Up to 100 µl nuclear extract (NE) buffer (Table 2.6) depending on the volume of CE buffer (half the volume of CE buffer) was added to the pellet to destroy the nuclear membrane and salt concentration was adjusted using up to 67 µl 5 M NaCl. Samples were sonicated using Sonifier UP50H (Hielscher Ultrasonics GmbH) for 0.5 cycle and 100% amplitude for 10 s and incubated on ice for 30 min. Preparations were centrifuged at maximum speed at 4°C for 10 min. The supernatant containing the nuclear protein was transferred into a clean tube. The protein samples were stored at -80°C.

Protein concentration was determined using bicinchoninic acid (BCA) assays. Protein samples were diluted 1:24 and 3:22 in H₂O in a 96-well-plate. 200 µl of BC Assay Working Reagent (50:1 BC Assay Working reagent A:BC Assay Working reagent B) were added and samples were incubated at 37°C for 30 min. Protein concentrations were measured at 563 nm using SynergyMx microplate reader (BioTek®). A standard curve with bovine albumin fraction V,

protease-free (BSA) dilutions of known protein concentrations (0-30 µg) was established and used to determine the protein concentration of samples. Protein concentrations were adjusted using either CE or NE buffer and measurement was repeated using 2:23 dilution. Samples were stored at -80°C.

2.2.5 SDS-PAGE and western blot analyses

In order to determine the effect of Curcumin and BA on important histone marks and stem-cell markers, sodium dodecyl sulfate-polyacrylamide gel electrophoresis (SDS-PAGE) were performed. Protein concentrations were adjusted with NE or CE buffer, and 1x LPP was added. Prepared samples were heated at 95°C for 5 min and either stored at -20°C or immediately used for SDS-PAGE.

Gels were prepared according to Table 2.11 depending on the size of target protein. Gels were run in the electrophoresis system (BioRad) in Laemmli running buffer (Table 2.6) by applying a voltage of 80 to 120 V. Molecular weight of the proteins was determined using a pre-stained protein ladder.

Table 2.11 Compositions of stacking and separating SDS-PAGE gels

SDS-polyacrylamide gel	Composition
Stacking gel 5.6%	14% Rotiphorese ® Gel 40 (29:1), 1X UT buffer, 0.1% APS, 0.1% TEMED
Separating gel 12%	30% Rotiphorese ® Gel 40 (29:1), 1X LT buffer, 0.1% APS, 0.1% TEMED
Separating gel 15%	37.5% Rotiphorese ® Gel 40 (29:1), 1X LT buffer, 0.1% APS, 0.1% TEMED
Separating gel 20%	50% Rotiphorese ® Gel 40 (29:1), 1X LT buffer, 0.1% APS, 0.1% TEMED

Separated proteins were transferred onto an Immobilon-P PVDF-membrane (Merck) using a wet blotting system (Biometra) at 500 mA for 45 min in blotting buffer (Table 2.6). Before blotting the Immobilon-P PVDF-membranes were activated in methanol for 1 min then placed in blot buffer.

After blotting, gels were stained with Coomassie staining solution (Table 2.6) overnight. Gels were subsequently bleached with Coomassie destaining solution (Table 2.6) three times for 20 min. Gels were placed in water for 24 to 72 h and photographed.

After blotting, membranes were blocked with blocking solution (Table 2.6) for 1 h at room temperature to prevent unspecific antibody binding. Membranes were then incubated with the primary antibody diluted in either 5% BSA or 5% powdered milk in TBST-T and incubated at 4°C overnight. Membranes were washed with TBST-T three times for 10 min and incubated with the matching secondary antibody diluted in either 5% BSA or 5% powdered milk at room temperature for 1 h and again washed with TBS-T three times for 10 min.

In order to detect the antibody-marked protein of interest, horseradish peroxidase ECL solution A and B were mixed 1:1 and applied to membranes. Chemiluminescence was measured using the Luminescent image analyzer LAS-4000 mini (Fujifilm).

2.2.6 Sphere formation assay

To study the effect of Curcumin and BA on stem cell-like properties, sphere formation assays were performed. For sphere formation assay, DIPG-007 and GBM-001 cells were seeded in 12-well-plates at a concentration of 5 000 cells/ml in 1 ml using TSM work (Table 2.1). Cells were incubated at 37°C for 5 h and treated with Curcumin or BA. After 96 h of incubation 1 ml TSM work medium (Table 2.1) with matching Curcumin or BA concentrations was added, and cells were incubated at 37°C for another 72 h. Ten% fetal calf serum (FCS) was added, and cells were incubated at 37°C until spheres attached to the bottom. One ml of Crystal Violet staining solution (Table 2.6) was added, and plates were placed on a shaker for 1 h. The staining solution was removed, and wells were gently washed with tap water. Plates were dried overnight at 37°C. Sphere formation ability was evaluated using the ImageJ tool “Particle analyzer”.

2.2.7 Colony formation assay

To investigate the effect of Curcumin and BA on clonogenicity, colony formation assays were performed. For colony formation assay, DIPG-007 and GBM-001 cells were seeded in 12-well-plates at a concentration of 5 000 cells/ml in 1 ml using TSM work medium (Table 2.1) with 10% FCS. Cells were incubated for 5 h and treated with Curcumin or BA. Since DIPG-007 cells exhibit a much faster proliferation than GBM-001 cells, they were stained with Crystal Violet staining solution (Table 2.6) after 96 h while 1 ml fresh medium containing matching Curcumin or BA concentrations was added to GBM-001 cells. GBM-001 cells were

cultured for another 72 h before staining with Crystal Violet (Table 2.6). Plates were placed on a shaker for 1 h. Crystal Violet staining solution was removed, and wells were gently washed with water. Plates were dried overnight at 37°C. Colonized area was evaluated using the ImageJ tool “ColonyArea”.

2.2.8 RNA isolation

For RNA isolation, DIPG-007 cells were seeded into 6-well-plates at a concentration of 50 000 cells/ml in 2 ml TSM work medium (Table 2.1). After 24 h of incubation at 37°C, cells were treated with Curcumin or BA and incubated at 37°C for another 48 h before harvest. For harvesting, cells were transferred into 15 ml falcon tubes, and wells were washed with PBS. Cells were centrifuged at 1 000 rpm for 5 min and the supernatant was removed. Pellets were frozen in liquid nitrogen and stored at -80°C.

RNA for RNA-seq was isolated using ReliaPrep™ RNA cell Miniprep System following manufacturer’s instructions. Samples were concentrated using ReliaPrep™ RNA Clean-Up and Concentration System according to manufacturer’s instructions. Concentration was determined using the spectrophotometer NanoDrop® ND-1000p (ThermoScientific) and concentrations were adjusted with nuclease free water. Samples were stored at -80°C.

RNA gels were run to exclude RNA degradation. One% Agarose was diluted in 1x TAE buffer and boiled until liquid was clear and agarose-ethidium-bromide-gels were poured. 1x DNA loading dye was added to 500 to 1 000 ng RNA and gels were run at 120 V for 5 min.

2.2.9 Library preparation, mRNA sequencing and data analysis

TruSeq RNA Library Prep Kit v2 (Illumina) was used according to the manufacturer’s instructions by the Transcriptome and Genome Analysis Laboratory (TAL) at the University Medical Center Göttingen to synthesize libraries from RNA. Pools of libraries were sequenced by the TAL using HiSeq4000 (Illumina, 50SE).

Candidate genes were filtered to a minimum of 0.75-fold change for upregulation and 1.5-fold change for downregulation with a false discovery rate (FDR)-corrected p-value<0.05. To analyze the gene ontology (GO-) annotation, the Database for Annotation, Visualization and Integrated Discovery (DAVID) Bioinformatics Resources 6.8 (Frederick, US) was used (Huang et al. 2009a, 2009b).

2.2.10 Statistical analysis

Statistical analysis was performed using Excel 2013.

Unless stated otherwise all experiments were performed in biological triplicates. The graphs in this study show the mean value normalized to the control with the respective standard error of the mean (SEM). To determine statistical significance, paired student's t-test was performed, p-values<0.05 were considered as statistically significant.

3 Results

3.1 Curcumin

Curcumin is one of the most commonly used CAM in patients with DIPG (El-Khouly et al. 2021) and has been reported to express various anti-cancer properties in different cancer types, amongst others in adult GBM (Gersey et al. 2017; Balasubramanyam et al. 2004; Xi et al. 2015; Yin et al. 2014). Therefore, the anti-cancer effects of Curcumin in pedHGG cells were investigated in this study.

3.1.1 Curcumin reduces cell viability in pedHGG cells in a dose dependent manner

Curcumin has been observed to decrease cell viability in adult GBM cells in a dose dependent manner (Gersey et al. 2017). Therefore, it was hypothesized that Curcumin reduces cell viability in pedHGG cells as well. To investigate the impact of Curcumin on the viability of pedHGG cells, MTT-cell viability assays were performed. The H3K27M-mutant cell line DIPG-007 and the control H3WT cell line GBM-001 were used to determine if Curcumin exerts H3K27M-mutation dependent effects on cell viability. To observe the different effects of Curcumin on CSC-like spheroid cells and on adherent monolayer cells, cells were cultured either under spheroid (TSM work medium, Table 2.1) or adherent monolayer conditions (TSM diff medium, Table 2.1).

Treatment with Curcumin reduced cell viability in a dose dependent manner. No statistically significant difference of cell viability between GBM-001 and DIPG-007 cells could be detected (Figure 1). Adherent monolayer cells, which resemble a more differentiated tumor phenotype, were more sensitive to treatment with Curcumin than spheroid cells, which resemble a more CSC-like tumor phenotype. For all concentrations higher than 22.2 μM Curcumin this effect was statistically significant in both cell lines (Figure 1). After treatment with 22.2 μM Curcumin spheroid GBM-001 cells expressed a cell viability of 35% which was five times higher than the cell viability expressed by the corresponding differentiated monolayer GBM-001 cells treated with the same concentration of Curcumin (Figure 1). In contrast, treatment of spheroid DIPG-007 cells with 22.2 μM Curcumin resulted in a reduction of cell viability to 49% compared to control while the cell viability of differentiated monolayer DIPG-007 cells was reduced to 12% of control after treatment with the same concentration of Curcumin (Figure 1).

The concentration at which 50% of the cells are non-viable (IC_{50}) were approximately $14.8 \mu\text{M}$ for GBM-001 cells and $22.2 \mu\text{M}$ for DIPG-007 cells under spheroid conditions (Figure 1).

After treatment with $50 \mu\text{M}$ of Curcumin, cell viability of both differentiated DIPG-007 and differentiated GBM-001 cells was reduced to 5% of control cells (Figure 1 A). Spheroid DIPG-007 and GBM-001 cells expressed a cell viability of 11% and 13% of control after treatment with $50 \mu\text{M}$ of Curcumin (Figure 1 B).

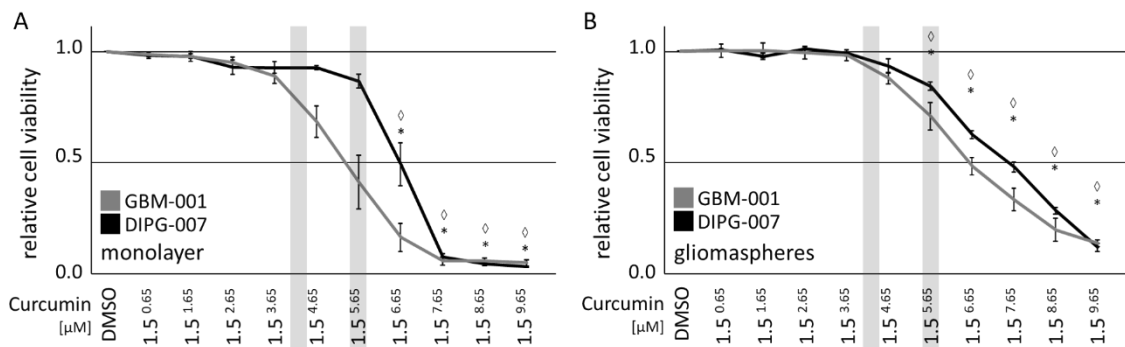


Figure 1: **Curcumin reduces cell viability in pedHGG cells in a dose dependent manner.** MTT-cell viability dilution curves of (A) pedHGG cells cultured under adherent monolayer conditions and (B) under spheroid conditions after treatment with increasing concentrations of Curcumin as indicated and incubation time of 72 h (DMSO control = 100%, \diamond /* $p < 0.05$; \diamond for DIPG-007 cells, * for GBM-001 cells). Grey bars indicate concentrations used for further experiments.

These results reveal that Curcumin reduces cell viability in pedHGG cells in a dose dependent manner.

To further investigate the effect of Curcumin on DIPG-007 and GBM-001 cells especially in combination with radiochemotherapy, concentrations of $5 \mu\text{M}$ and $10 \mu\text{M}$ Curcumin were used for following experiments. After treatment with $10 \mu\text{M}$ Curcumin cell viability was already reduced to approximately 70% compared to control hence suggesting that cell functions were impaired while treatment with $5 \mu\text{M}$ Curcumin resulted in no relevant reduction of cell viability (Figure 1).

3.1.2 Curcumin sensitizes GBM-001 cells to temozolomide

The most commonly performed therapy for patients with DIPG consists of radiochemotherapy with the chemotherapeutic agent TMZ (El-Khouly et al. 2019). The combination of Curcumin with TMZ or irradiation led to increased therapeutic efficacy in adult GBM (Yin et al. 2014; Meng et al. 2017). Therefore, it was hypothesized that Curcumin

influences treatment with TMZ and/or irradiation in DIPG-007 and GBM-001 cells. To investigate the effect of Curcumin on TMZ radiochemotherapy, MTT-cell viability assays in combination with TMZ or irradiation, respectively, or a combination of both were performed. PedHGG cells were cultured under spheroid conditions (TSM work medium, Table 2.1) since spheroid cells expressed a higher resistance towards treatment with Curcumin compared to adherent monolayer cells (Figure 1).

Treatment with 10 μ M Curcumin reduced cell viability in both DIPG-007 and GBM-001 cells significantly to 86% and 66%, respectively (Figure 2).

Irradiation decreased cell viability to comparable levels of 70% in DIPG-007 and 64% in GBM-001 cells. Combination of irradiation with 10 μ M Curcumin led to further reduction of cell viability in both cell lines compared to control (Figure 2). Treatment with Curcumin and irradiation had an additive effect in DIPG-007 cells (Figure 2 A).

Single treatment with 10 μ M TMZ had no significant effect on cell viability in both pedHGG cell lines as compared to control. However, combination of 10 μ M TMZ with 10 μ M Curcumin decreased cell viability of DIPG-007 cells to 83% and of GBM-001 cells to 44% as compared to control while single treatment with 10 μ M Curcumin reduced cell viability to 86% in DIPG-007 cells and to 66% in GBM-001 cells (Figure 2). Of note, treatment with Curcumin showed no sensitizing effect on TMZ treatment in DIPG-007 cells (Figure 2 A). In contrast, 10 μ M Curcumin sensitized GBM-001 cells to TMZ treatment (Figure 2 B).

Combined therapy of 10 μ M TMZ with 8 Gy irradiation reduced cell viability of DIPG-007 and GBM-001 cells to 67% and 64%, respectively, as compared to control treated cells (Figure 2). Additional treatment with 10 μ M Curcumin reduced cell viability of both cell lines further to 58% in DIPG-007 and 44% in GBM-001 cells. However, no sensitizing effect was observed. (Figure 2).

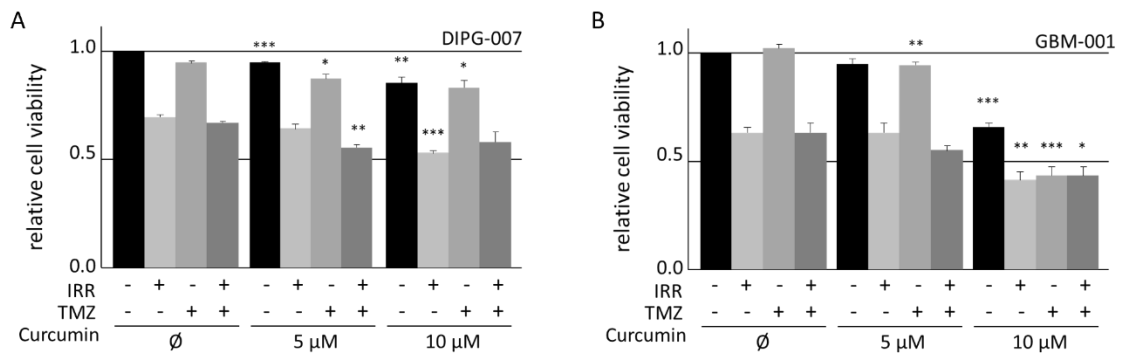


Figure 2: **Curcumin sensitizes GBM-001 cells to treatment with TMZ.** MTT-cell viability assays of (A) DIPG-007 and (B) GBM-001 cells after treatment with Curcumin and 10 μ M TMZ (day 1 and day 3), in combination with irradiation (day 2), as indicated. Relative cell viability was assessed after 5 d of incubation (DMSO control, 0 Gy = 100%, * $p < 0.05$, ** $p < 0.01$, *** $p < 0.005$ with respect to non-Curcumin treated \emptyset -control cells).

These results suggest that Curcumin displays positive effects on standard therapy and sensitizes GBM-001, but not DIPG-007 cells to treatment with TMZ.

3.1.3 Curcumin reduces H3K27- and H4K8-acetylation in DIPG-007, but not in GBM-001 cells

More than 85% of DIPG carry a H3K27M-mutation which leads to changes in the epigenetic landscape with an increase of H3K27ac and a decrease of H3K27me3 (Castel et al. 2018; Schwartzenruber et al. 2012). It had been previously reported that Curcumin inhibits the histone acetyl transferase (HAT) CBP which induces acetylation at histone 3 and 4 (Lu et al. 2014). Hence, it was proposed in the present study that Curcumin may also influence the epigenetic landscape in DIPG cells by affecting histone acetylation.

To examine the effect of Curcumin on histone modifications, western blot analyses with antibodies against H3K27me3, H3K27ac and H4K8-acetylation (H4K8ac) were performed. H3K27M-mutant DIPG-007 and, as a control, H3WT GBM-001 cells were cultured as glioma spheres under stemness culture conditions and treated with 5 μ M or 10 μ M Curcumin, respectively.

While treatment with Curcumin only slightly reduced H3K27ac and had no significant effect on H4K8ac levels in H3WT GBM-001 cells, treatment with Curcumin significantly reduced H3K27ac and H4K8ac levels in H3K27M-mutant DIPG-007 cells (Figure 3).

In contrast, treatment with Curcumin did not influence H3K27me3 levels in DIPG-007 or GBM-001 cells (Figure 3).

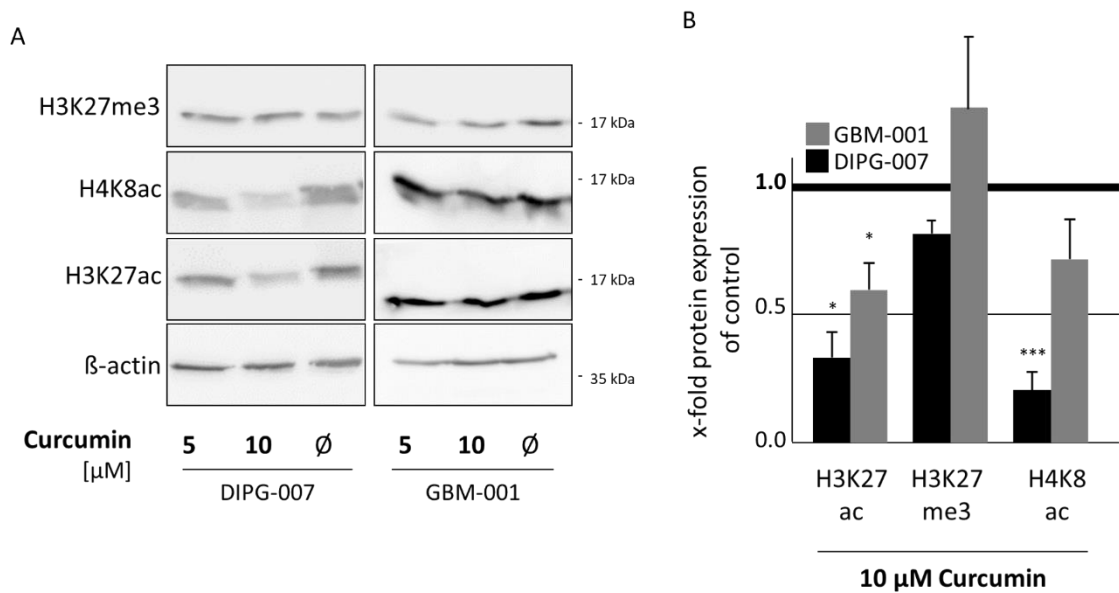


Figure 3: Curcumin reduces H4K8ac and H3K27ac in DIPG-007 cells in a dose dependent manner. (A) Western blot analyses of nuclear protein fraction of DIPG-007 and GBM-001 cells with antibodies against H3K27me3, H4K8ac and H3K27ac after treatment with 5 μ M and 10 μ M Curcumin, as indicated. (B) Quantification of protein expression after treatment with 10 μ M Curcumin compared to DMSO control (* $p < 0.05$, ** $p < 0.01$, *** $p < 0.005$ with respect to respective non-Curcumin treated \emptyset -control cells). β -actin served as control.

These results suggest that Curcumin influences the epigenetic landscape and reduces histone acetylation in H3K27M-mutated DIPG-007 cells stronger than in H3WT GBM-001 cells.

3.1.4 Curcumin reduces clonogenicity in DIPG-007 cells and proliferation in pedHGG cells

Curcumin was observed to inhibit growth and clonogenicity in adult GBM cells (Gersey et al. 2017; Xu et al. 2018). Furthermore, it has been observed that adherent monolayer cells are more sensitive towards drug treatment than CSC-like spheroid cells (Meel et al. 2017). Therefore, the influence of Curcumin on clonogenic functions in pedHGG cells was investigated.

To investigate the effect of Curcumin on stemness, sphere formation assays were performed. DIPG-007 and as control GBM-001 cells were cultured under spheroid conditions (TSM work medium, Table 2.1) and treated with 5 μ M or 10 μ M Curcumin respectively.

H3K27M-mutated DIPG-007 cells had a 8.5-times higher sphere forming capacity than H3WT GBM-001 cells after 7 d of incubation (Figure 4 A)

All over, treatment with Curcumin reduced the number of large spheres (more than 100 μm in diameter) in both cell lines (Figure 4 A, B). Treatment with 5 μM of Curcumin increased the number of small spheres but reduced the total amount of spheres in DIPG-007 cells significantly (Figure 4 A). The number of spheres formed by DIPG-007 cells treated with 10 μM of Curcumin was reduced to 524 representing a reduction of 33% as compared to control (Figure 4 A). No statistically significant effect was observed in GBM-001 cells treated with 5 μM Curcumin; but treatment with 10 μM Curcumin reduced the number of spheres formed by GBM-001 cells significantly by 26% as compared to control (Figure 4 A).

Since strong reduction of number of spheres was observed in DIPG-007 cells, expression levels of the stemness marker Oct 4 was investigated to determine if Curcumin may influence stemness potential by changing expression of this stemness related protein. Indeed, Curcumin decreased Oct 4 protein levels in DIPG-007 cells in a dose dependent manner (Figure 4 C).

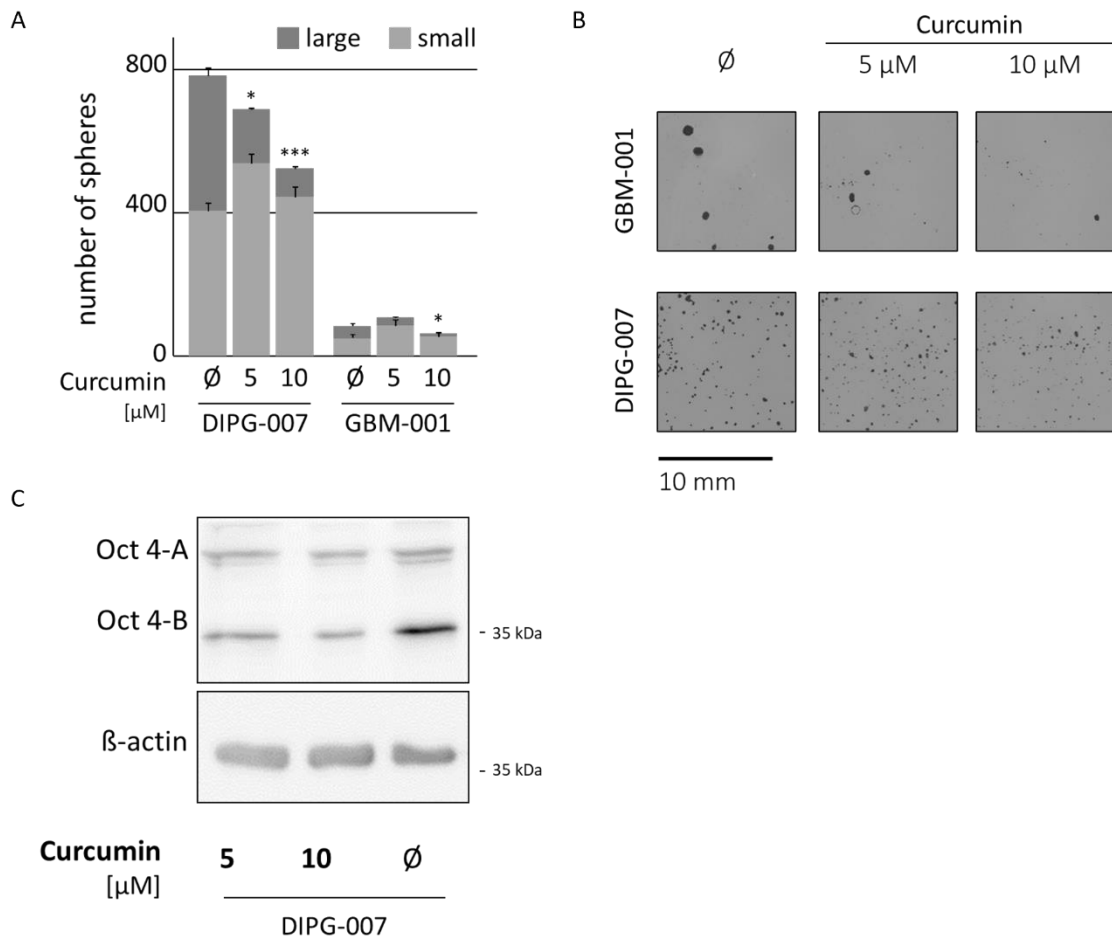


Figure 4: Curcumin reduces sphere formation ability and stemness-marker expression in DIPG-007 cells. (A, B) Sphere formation ability of DIPG-007 and GBM-001 cells after 7 d of incubation with 5 μM and 10 μM Curcumin, as indicated. (A) Absolute number of spheres (small spheres 50 -100 μM in diameter, large spheres > 100 μM in diameter; * $p < 0.05$, ** $p < 0.01$, *** $p < 0.005$ with respect to non-Curcumin treated ∅-control cells). (B) Representative brightfield images of spheres of DIPG-007 and GBM-001 cells after treatment with 5 μM and 10 μM Curcumin, as indicated. (C) Western blot analyses of nuclear protein fraction of DIPG-007 cells with antibodies against Oct 4 after treatment with 5 μM and 10 μM Curcumin, as indicated. β-actin served as loading control.

In order to examine the effect of Curcumin on self-renewal and proliferation in pedHGG cells under differentiating conditions, colony formation assays were performed. PedHGG cells were cultured under adherent monolayer conditions which resemble a more differentiated phenotype (TSM work medium with 10% FCS, Table 2.1) and treated with Curcumin.

Treatment with Curcumin led to a reduction of colonized area in a dose dependent manner of both, DIPG-007 and GBM-001 cells (Figure 5). Treatment with 10 μM Curcumin reduced the

colonized area to 27.5% in DIPG-007 cells after 4 d and to 27.9% in GBM-001 cells after 7 d compared to control treated pedHGG cells (Figure 5 A).

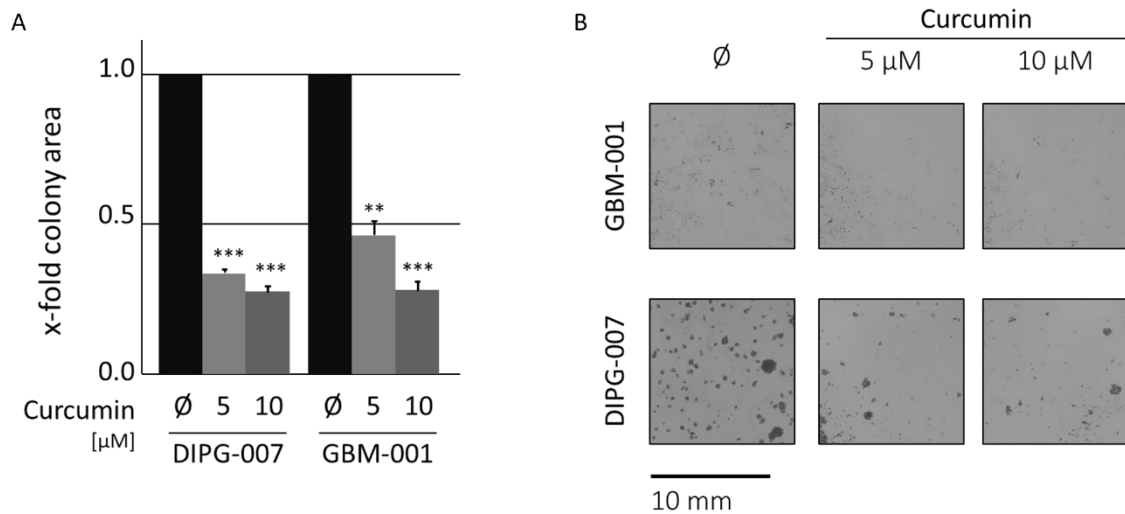


Figure 5: **Curcumin reduces colony formation ability in pedHGG cells.** (A, B) Colony formation capability of DIPG-007 cells after 4 d and GBM-001 cells after 7 d of incubation with 5 μM and 10 μM Curcumin, as indicated. (A) Analysis of the relative colonized area of pedHGG cells after treatment with 5 μM and 10 μM Curcumin, as indicated * $p < 0.05$, ** $p < 0.01$, *** $p < 0.005$ with respect to non-Curcumin treated ∅-control cells). (B) Representative brightfield images of colonies of DIPG-007 and GBM-001 cells after treatment with 5 μM and 10 μM Curcumin, as indicated.

In summary, Curcumin reduces clonogenicity of pedHGG cells and reduces stemness-associated marker expression in DIPG-007 cells on protein level.

3.1.5 Curcumin induces cell cycle arrest and apoptosis in DIPG-007 cells

To gain further insight into the molecular mechanisms regulated by Curcumin in DIPG cells, RNA-seq was performed to determine the transcriptome upon Curcumin treatment. Treatment with Curcumin influenced the epigenetic marks H3K27ac and H4K8ac in DIPG-007 and GBM-001 cells (Figure 3). Since epigenetic marks are associated with gene activation and silencing, it was investigated whether the epigenetic changes induced by Curcumin alter the transcriptome. The epigenetic effect had been stronger in DIPG-007 cells than in control GBM-001 cells. Therefore, RNA-seq was only performed in DIPG-007 cells.

A total of 1 158 transcripts were significantly altered after treatment with 10 μM Curcumin. 182 genes were >1.5-fold upregulated ($p < 0.05$) and 976 genes were <0.75-fold downregulated ($p < 0.05$). To determine potential biological effects of Curcumin, GO-

enrichment analyses were performed using the DAVID (Huang et al. 2009a). The 20 most enriched GO-annotations for 0.75-fold downregulated, and 1.5-fold upregulated pathways were determined (Figure 6). Of note, 19 of the 20 downregulated pathways after Curcumin treatment in DIPG-007 cells were associated with cell cycle and cell division (Figure 6 A). The two strongest upregulated pathways were associated with the p53-pathway and ferroptosis which are both associated with cell cycle arrest and cell death (Figure 6 B).

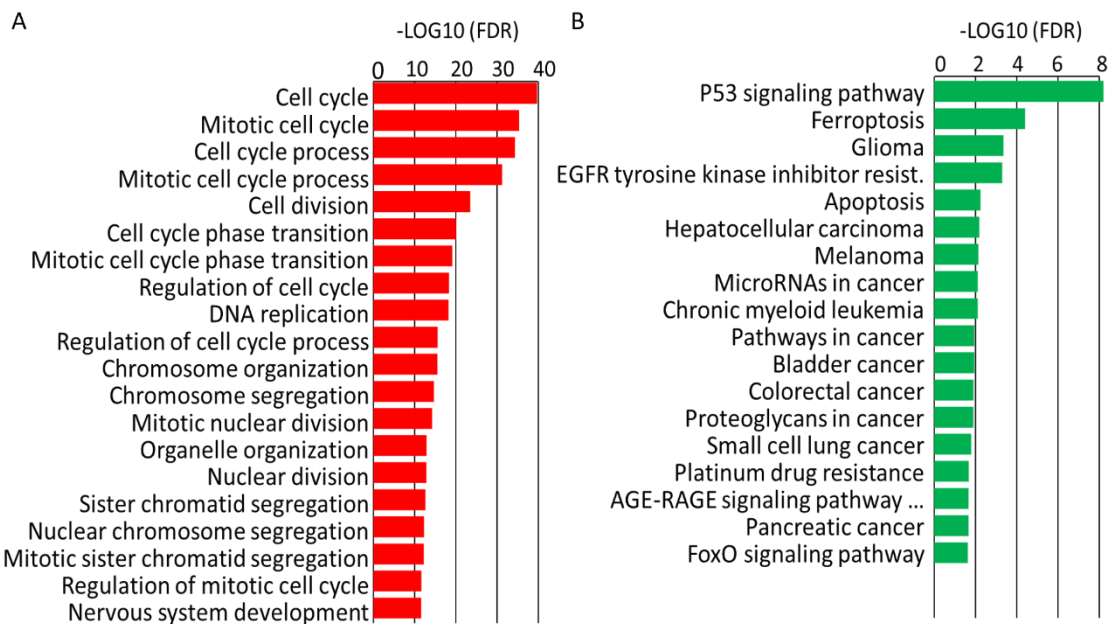


Figure 6: **Curcumin influences the cell cycle and induces apoptosis in DIPG-007 cells.** TOP20-GO-pathways enriched after treatment with 10 μ M Curcumin for 48 h ($\text{padjust} > 0.05$) of the (A) 0.75-fold down and (B) 1.5-fold upregulated genes.

The Kyoto Encyclopedia of Genes and Genomes (KEGG) pathways provides numerous pathway maps and associated genes. KEGG pathway analysis regarding the genes regulated by Curcumin showed that Curcumin downregulated many genes which are involved in cell cycle progression (Figure 7 B).

Furthermore, KEGG analyses of upregulated genes following Curcumin treatment indicated that Curcumin upregulated genes are involved in apoptosis, especially by the p53 signaling pathway (Figure 7 A).

To further confirm that Curcumin induces apoptosis in pedHGG cells, western blots probed with antibodies against the apoptosis marker Cleaved Caspase 3 were performed after treatment of pedHGG cells with 5 μM and 10 μM Curcumin.

Treatment with Curcumin resulted in a dose dependent increase of the apoptosis marker Cleaved Caspase 3 in DIPG-007 but not in GBM-001 cells (Figure 8).

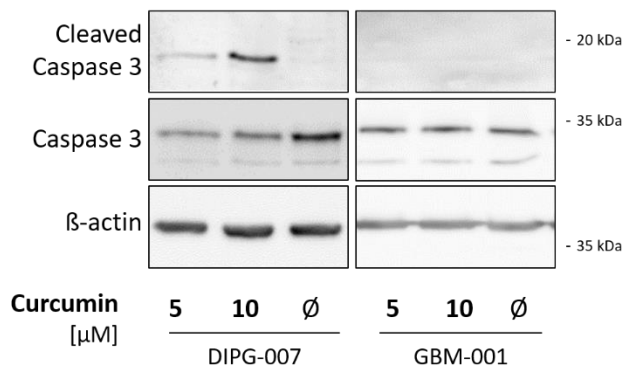


Figure 8: **Curcumin increases Cleaved Caspase 3 levels in DIPG-007 cells.** Western blot analyses of the cytoplasmatic protein fraction of DIPG-007 and GBM-001 cells with antibodies against Cleaved Caspase 3 and Caspase 3 after treatment with 5 μM and 10 μM of Curcumin, as indicated (n=2). β -actin served as control.

These results suggest that treatment with Curcumin inhibits cell cycle progression and induces apoptosis in DIPG-007 cells, but most likely not in GBM-001 cells.

3.2 Boswellic acids

Like Curcumin, BA are among the most commonly used CAM in patients with DIPG (El-Khouly et al. 2021). Even though BA have been reported to express various anti-cancer properties in adult GBM-cells (Conti et al. 2018; Schneider and Weller 2016), their effects in pedHGG cells had never been examined before. Therefore, the effect of α -BA, β -BA and AKBA in pedHGG cells was investigated in this study. The H3K27M-mutant DIPG-007 cell line and the control H3WT GBM-001 cell line were used, to examine whether BA exert any H3K27M-mutation dependent effects.

3.2.1 AKBA reduces cell viability most efficiently in pedHGG cells

It was reported that BA reduced cell viability in various cancer cells amongst others in adult GBM (Conti et al. 2018). Therefore, it was hypothesized that BA reduce cell viability in DIPG-007 and GBM-001 cells. To evaluate cytotoxic effects of α -BA, β -BA and AKBA on cell viability and to determine the most efficient BA, MTT-cell viability assays were performed. DIPG-007 and GBM-001 cells were cultured under either spheroid or adherent monolayer conditions to investigate if the three BA display different effects in the more under different culture conditions.

All three BA reduced cell viability of pedHGG cells at high concentrations. Adherent monolayer pedHGG cells were more sensitive to treatment with α -BA than spheroid cells (Figure 9 A, B). In addition, GBM-001 but not DIPG-007 adherent monolayer cells were more sensitive to treatment with β -BA than spheroid cells (Figure 9 C, D). But no significant difference of cell viability between adherent monolayer and spheroid cells could be detected after treatment with AKBA (Figure 9 E, F).

Treatment with α -BA influenced cell viability in both DIPG-007 and GBM-001 cells. Of note, up to a dosage of 8.89 μ M, α -BA increased cell viability of DIPG-007 cells under spheroid conditions significantly (Figure 9 B). Treatment with β -BA increased cell viability of DIPG-007 spheroid cells at maximum concentrations up to 13.34 μ M (Figure 9 D). However, this effect could not be observed in non-CSC-like pedHGG or GBM-001 spheroid cells (Figure 9). Higher concentrations of both α -BA and β -BA decreased cell viability in both pedHGG cell lines (Figure 9 A, B, C, D). In contrast, AKBA decreased cell viability of both DIPG-007 and GBM-001 cells in a dose dependent manner (Figure 9 E, F).

Treatment with AKBA led to no significant difference between cell viability of DIPG-007 and GBM-001 cells (Figure 9 E, F). However, apart from the increase of cell viability of DIPG-007 spheroid cells after treatment with low concentrations of α -BA and β -BA no statistically

significant difference of cell viability between DIPG-007 and GBM-001 cells were detected. (Figure 9).

AKBA had the strongest cell viability reducing effect in DIPG-007 and GBM-001 cells, followed by treatment with α -BA, while treatment with β -BA appeared as the least effective (Figure 9).

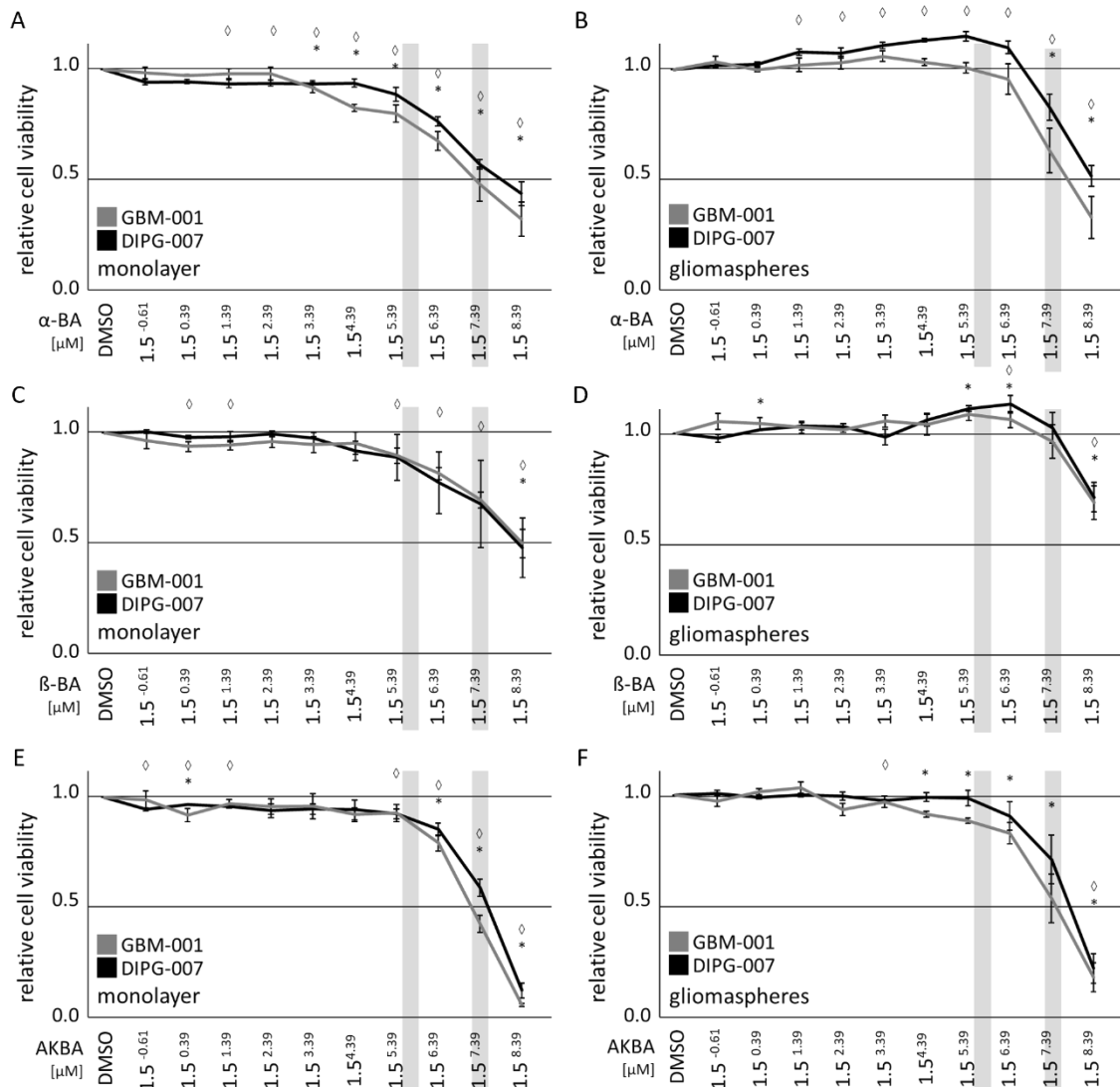


Figure 9: **AKBA reduces cell viability in pedHGG cells in a dose dependent manner.** MTT-cell viability dilution curve of pedHGG cells cultured under (A, C, E) adherent monolayer and (B, D, F) spheroid conditions with increasing concentrations of BA, as indicated. Relative cell viability of pedHGG cells after 72 h incubation time and treatment with increasing concentrations of (A, B) α -BA, (C, D) β -BA and (E, F) AKBA (DMSO control = 100%, \diamond /* $p < 0.05$; \diamond for DIPG-007 cells, * for GBM-001 cells). Grey bars indicate concentrations used for further experiments.

In summary, all three BA reduced cell viability of both DIPG-007 and GBM-001 cells after treatment with high concentrations of BA. AKBA decreased cell viability in a dose dependent manner. However, treatment with lower concentrations of α -BA and β -BA led to an increase of cell viability in DIPG-007 cells.

To evaluate the effect of α -BA, β -BA and AKBA in further experiments with radiochemotherapy, concentrations of 10 μ M and 20 μ M BA were determined.

3.2.2 Boswellic acids increase the cell viability reducing effect of temozolomide in pedHGG cells

The most commonly performed treatment of patients with DIPG consists of irradiation in combination with the chemotherapeutic TMZ (El-Khouly et al. 2019). It was shown that BA positively influence radiochemotherapy in adult GBM cells (Conti et al. 2018; Schneider and Weller 2016). To examine the effect of BA on radiochemotherapy in DIPG-007 and GBM-001 cells, MTT-cell viability assays were performed in combination with TMZ and/or irradiation.

Treatment with 10 μ M TMZ did not influence cell viability of neither DIPG-007 nor GBM-001 cells. When 10 μ M TMZ was combined with 10 μ M of α -BA, β -BA, or AKBA only AKBA had an additive reducing effect on cell viability in DIPG-007 cells (Figure 10 E). However, cell viability after treatment with 10 μ M TMZ combined with 20 μ M of α -BA, β -BA or AKBA in GBM-001 cells was significantly decreased (Figure 10 B, D, F). While combination of 10 μ M TMZ with 20 μ M α -BA, β -BA or 10 μ M AKBA further decreased cell viability of DIPG-007 cells as well, this effect was stronger in GBM-001 than in DIPG-007 cells (Figure 10). Treatment with 20 μ M β -BA or AKBA sensitized GBM-001 cells to TMZ (Figure 10 D, F). Overall, β -BA had the strongest supportive impact of all BA on TMZ treatment and reduced cell viability of GBM-001 cells to 58% as compared to control (Figure 10 D).

Irradiation reduced cell viability of both GBM-001 and DIPG-007 cells by approximately 30%. No significant decrease of cell viability was detected after irradiation therapy and 10 μ M of α -BA, β -BA or AKBA (Figure 10). However, combination of 20 μ M α -BA significantly increased the cell viability reducing effect of irradiation, in both GBM-001 and DIPG-007 cells (Figure 10 A, B). In addition, combination of 20 μ M AKBA and irradiation further reduced cell viability of DIPG-007 cells (Figure 10 E). In combination with irradiation, neither 10 μ M nor 20 μ M β -BA had a statistically significant impact on cell viability in either cell line (Figure 10 C, D).

Combination of TMZ and irradiation had no significantly stronger impact on cell viability than irradiation alone. Addition of 10 μM α -BA or AKBA to TMZ and irradiation further decreased cell viability of DIPG-007 but not GBM-001 cells (Figure 10). Furthermore, cell viability of DIPG-007 cells was further decreased in a significant way after addition of 20 μM α -BA or AKBA to TMZ and irradiation (Figure 10 A, E). Neither 10 μM nor 20 μM β -BA combined with irradiation and TMZ had a statistically significant impact on cell viability in either cell line (Figure 10 C, D).

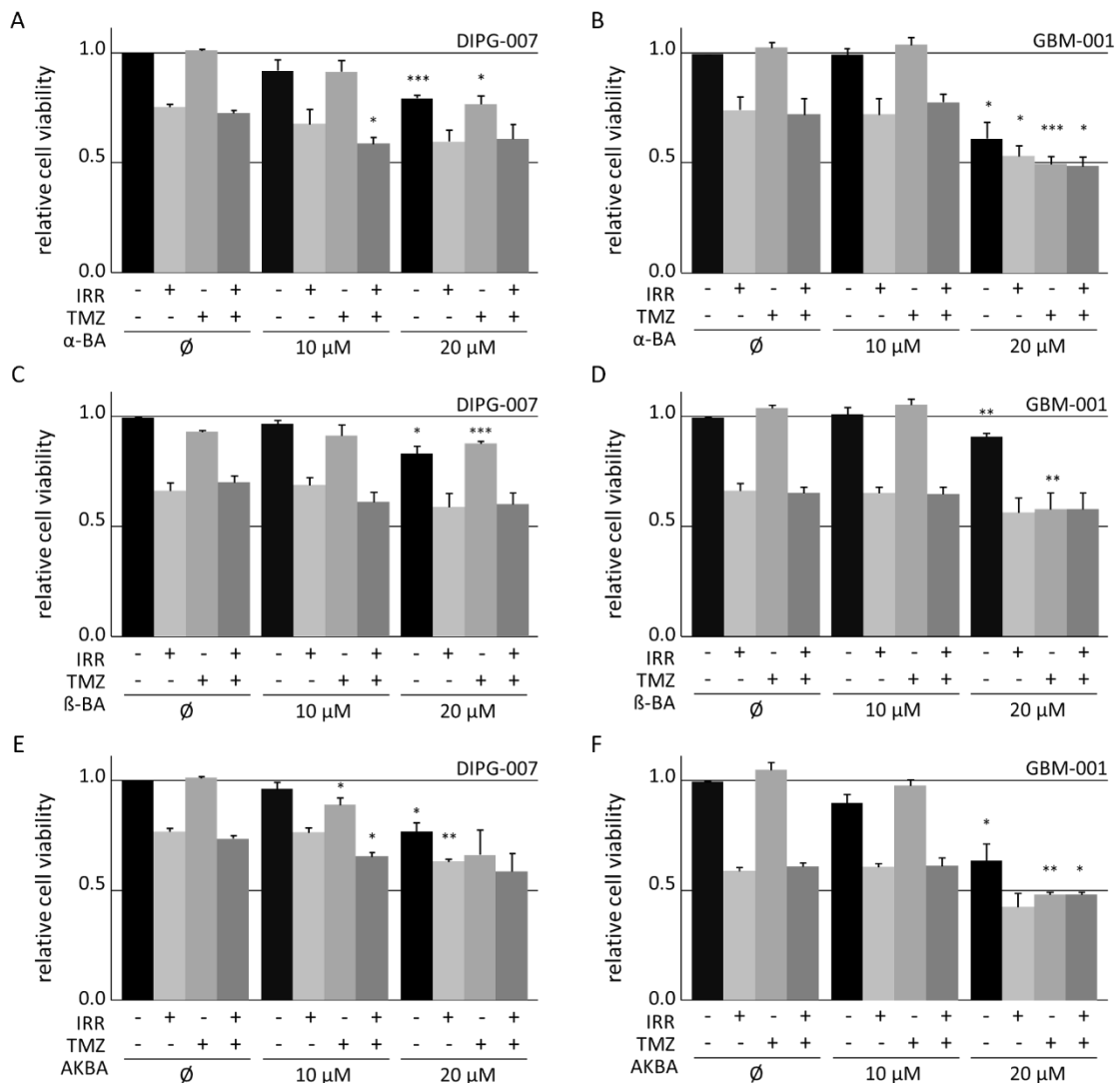


Figure 10: **BA increase the cell viability reducing effect of TMZ in pedHGG cells.**

MTT-cell viability assay of (A, C, E) DIPG-007 and (B, D, F) GBM-001 cells after treatment with BA and 10 μM TMZ (day 1 and day 3), in combination with irradiation (day 2), as indicated. Relative cell viability was assessed three further days after treatment with (A, B) α -BA, (C, D) β -BA and (E, F) AKBA (DMSO control, 0 Gy = 100%, * p < 0.05, ** p < 0.01, *** p < 0.005 with respect to respective non-BA treated Ø-control cells).

These results suggest that α -BA, β -BA and AKBA sensitize GBM-001 cells to TMZ. In addition, combination of TMZ with BA has a cell viability decreasing effect in DIP-007 cells but not as strong as in GBM-001 cells. Furthermore, α -BA and AKBA seem to have a positive impact on irradiation treatment alone or in combination with TMZ in all pedHGG cells, while β -BA does not have any statistically significant cell viability effect with irradiation alone or in combination with TMZ.

3.2.3 Boswellic acids show no effects on histone modifications in pedHGG cells

The H3K27M-mutation and subsequent changes in the epigenetic landscape, namely reduction of H3K27me3 and increase of H3K27ac, are present in 85% of DIPG (Castel et al. 2018). Therefore, the influence of BA on these histone modifications was investigated in H3K27M-mutant DIPG-007 cells. To investigate the effect of BA on histone modifications, western blot analyses evaluating H3K27me3, H3K27ac and H4K8ac were performed.

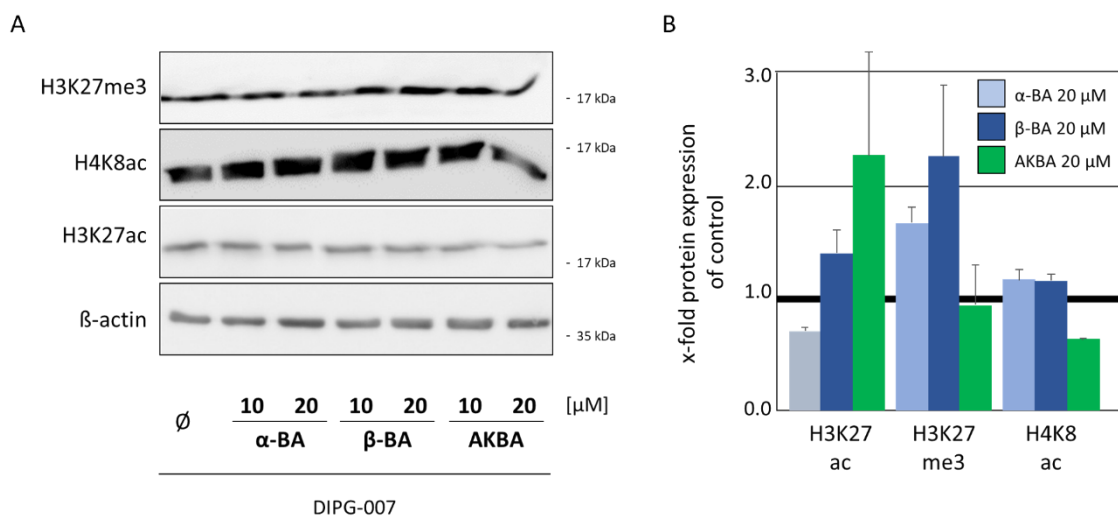


Figure 11: **BA have no effect on epigenetic histone modifications.** (A) Western blot analyses of the nuclear protein fractions of DIPG-007 cells with antibodies against H3K27me3, H4K8ac and H3K27ac after 72 h treatment with 10 μ M and 20 μ M α -BA, β -BA and AKBA, as indicated. β -actin served as loading control (n=2). (B) Quantification of proteins after treatment with 20 μ M α -BA, β -BA and AKBA compared to DMSO control.

Quantification of protein expression suggest a slight decrease of H3K27ac after treatment with 20 μ M α -BA and a slight decrease of H4K8ac after treatment with 20 μ M AKBA. To note, this subset of experiments had been only performed in duplicates. No effect on any of the other chosen histone modifications H3K27me3, H3K27ac or H4K8ac could be observed after treatment with α -BA, β -BA and AKBA (Figure 11).

In summary, BA treatment does not seem to alter epigenetic marks on histone 3 and 4 in DIPG-007 cells.

3.2.4 Boswellic acids reduce clonogenicity in dependence on the phenotype and cell line

It has been reported that BA reduce clonogenicity in adult GBM (Conti et al. 2018; Schneider and Weller 2016). Therefore, it was hypothesized that BA reduce clonogenicity in pedHGG cells. To examine the impact of α -BA, β -BA and AKBA on clonogenicity, colony and sphere formation assays were performed.

To evaluate the effect of α -BA, β -BA and AKBA on proliferation and self-renewal, colony formation assays were performed. PedHGG cells were cultured under adherent monolayer conditions which resemble a more differentiated phenotype (TSM work medium with 10% FCS, Table 2.1) and treated with α -BA, β -BA or AKBA. Since DIPG-007 cells grow much faster, the colonized area was evaluated after 96 h for DIPG-007 cells. The control GBM-001 cells were incubated for additional 72 h before evaluating colonized area.

The colonized area of DIPG-007 cells after treatment with both 10 μ M and 20 μ M α -BA, β -BA or AKBA was reduced in a dose dependent manner (Figure 12). Among all BA, treatment with AKBA resulted in the strongest reduction of colonized area (Figure 12 A). While DIPG-007 cells showed a highly significant reduction of colonized area after treatment with 20 μ M α -BA, β -BA, or AKBA this effect could not be observed in GBM-001 cells, which did not show any response to BA treatment at all (Figure 12 A). Further treatment with 20 μ M α -BA even increased the capability of GBM-001 cells to form colonies significantly (Figure 12 A).

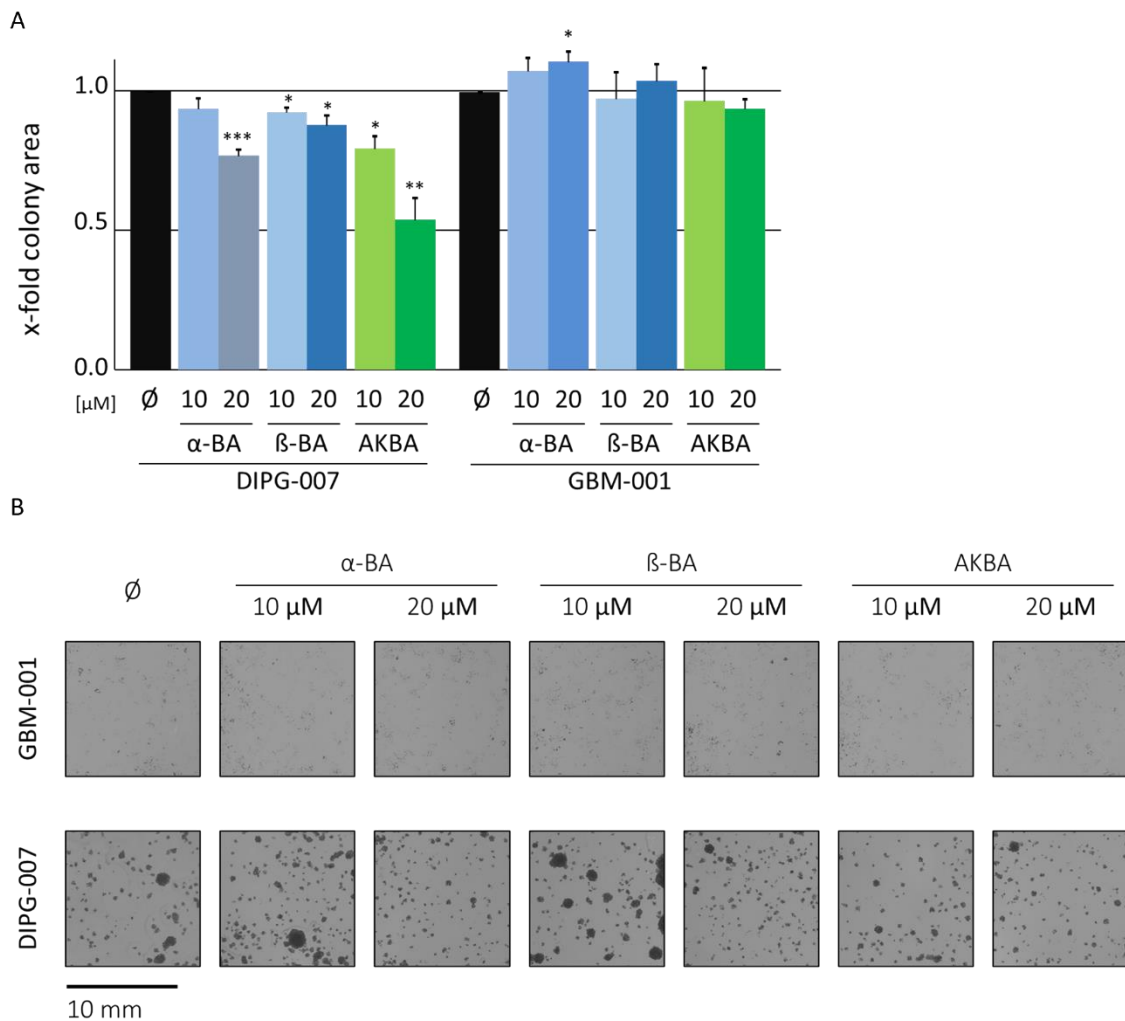


Figure 12: BA reduce colony formation ability in DIPG-007 cells. (A, B) Colony formation capability of DIPG-007 cells after 4 d and GBM-001 cells after 7 d of incubation with 10 μM and 20 μM α -BA, β -BA or AKBA, as indicated, of DIPG-007 and GBM-001 cells. (A) Analysis of the relative colonized area of pedHGG cells after treatment with 10 μM and 20 μM α -BA, β -BA or AKBA, as indicated * $p < 0.05$, ** $p < 0.01$, *** $p < 0.005$ with respect to non-BA treated \emptyset -control cells). (B) Representative brightfield images of colonies formed by DIPG-007 and GBM-001 cells after treatment with 10 μM and 20 μM α -BA, β -BA or AKBA, as indicated.

To analyze the ability to form spheres, sphere formation assays after treatment with α -BA, β -BA, or AKBA were performed.

DIPG-007 cells showed a 8.5-times higher capability to form spheres than GBM-001 cells (Figure 13 A). However, no statistically significant reduction of sphere numbers was observed in neither DIPG-007 nor GBM-001 cells after treatment with 10 μM or 20 μM α -BA, β -BA or AKBA (Figure 13). Moreover, 10 μM β -BA, and – to an even greater extend – 20 μM β -BA

increased the ability to form spheres in DIPG-007 and also slightly in GBM-001 cells (Figure 13 A).

An increase of small spheres and a decrease of large spheres in DIPG-007 cells after treatment with α -BA, β -BA, or AKBA could be observed (Figure 13 A). This effect could not be observed in GBM-001 cells after treatment with α -BA, β -BA, or AKBA (Figure 13 A).

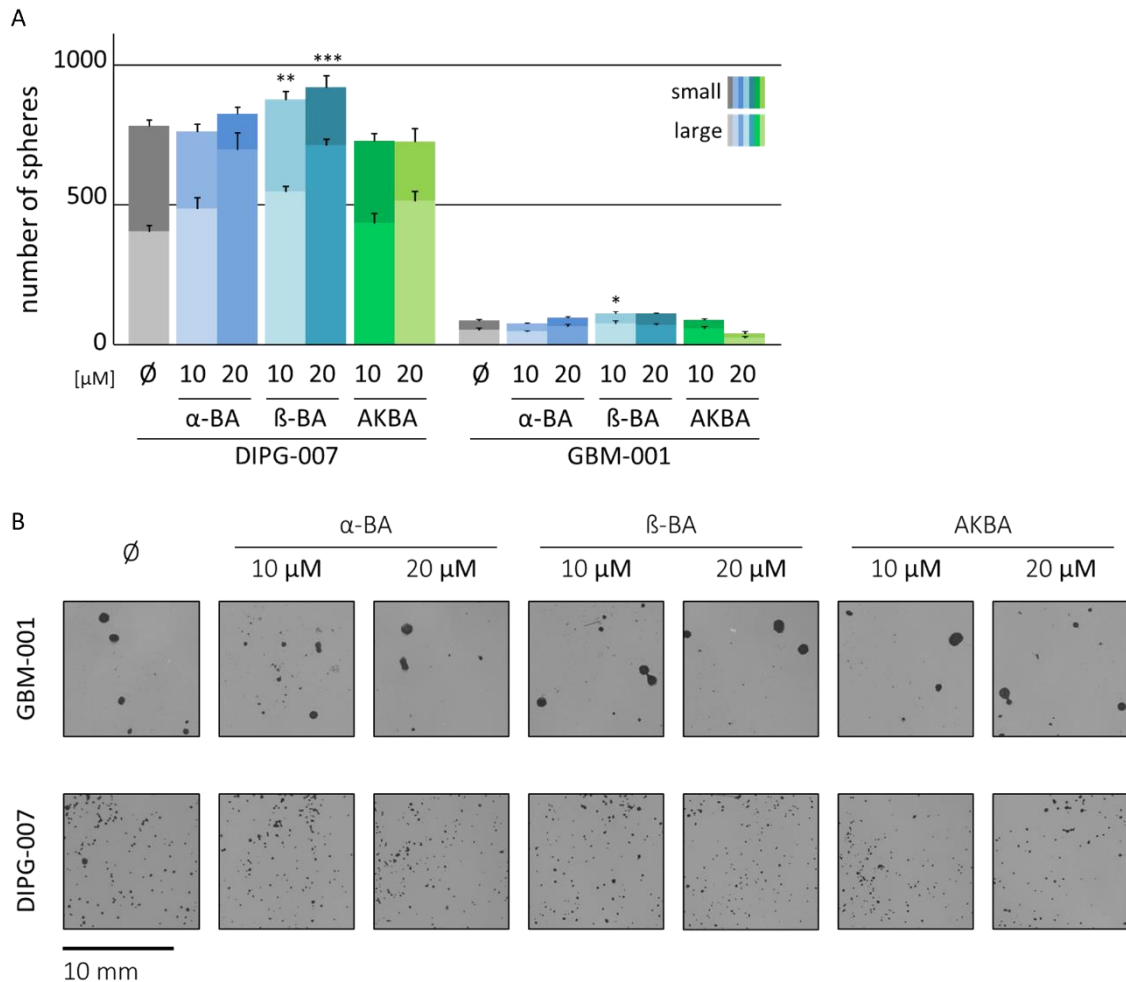


Figure 13: **β -BA induces sphere formation ability in pedHGG cells.** (A, B) Sphere formation ability in DIPG-007 and GBM-001 cells after 7 d of incubation with 10 μ M and 20 μ M α -BA, β -BA, or AKBA, as indicated. (A) Absolute number of spheres (small spheres 50-100 μ M in diameter, large spheres > 100 μ M in diameter; * p < 0.05, ** p < 0.01, *** p < 0.005 with respect to non-BA treated \emptyset -control cells). (B) Representative brightfield images of spheres.

These results suggest that α -BA, β -BA, and AKBA reduce the colony formation ability in DIPG-007 but not GBM-001 cells but do not reduce the sphere formation ability of both pedHGG cells. In contrary, β -BA seems to even induce sphere formation ability of pedHGG cells.

3.2.5 AKBA has no effect on gene transcription

To address the question as to whether treatment with BA influences transcription in DIPG cells, RNA-seq was performed with DIPG-007 cells cultured under spheroid conditions (TSM-work, Table 2.1). Since AKBA appeared to be the most effective of the three BA, RNA-seq was performed after treatment with 20 μ M AKBA.

Treatment with AKBA did not result in a significant change of any gene suggesting that AKBA does not at all influence transcription of genes in DIPG-007 cells (data not shown).

4 Discussion

DIPG are aggressive pedHGG with a median survival of 11 months after diagnosis (Hoffman et al. 2018). Currently, there is no cure available for affected patients and the available treatment options consisting of TMZ in combination with irradiation has not changed the overall dismal prognosis so far (Filbin and Suva 2016). Consequently, there is an urgent need for new therapeutic options. Since there are no effective therapies available, parents often access complementary treatment options such as Curcumin and BA (El-Khouly et al. 2021). Both, Curcumin and BA have been observed to express various anti-cancer properties amongst others in adult GBM cells (Conti et al. 2018; Gersey et al. 2017; Schneider and Weller 2016). The data evaluating the effect of these agents in pedHGG *in vitro* and *in vivo* is nevertheless limited. Hence, the aim of this study was to investigate the effect of Curcumin and BA *in vitro* to determine if they might be useful as complementary therapeutic options for children with DIPG.

85% of all DIPG carry a mutation in the *H3F3A* gene, encoding histone H3.3, or *HIST1H3B* genes, encoding histone H3.1, leading to the substitution of lysine 27 to methionine (mutation: H3K27M) (Castel et al. 2015). This mutation increases the stem cell-like potential, proliferation activity, and the therapeutic resistance of pedHGG cells (Wiese et al. 2020) and decreases the survival rate of patient with a non-thalamic-midline tumor (Castel et al. 2018). Thus, the present study was performed with a H3K27M-mutant DIPG and, as a control, a H3WT GBM cell line to evaluate if Curcumin and BA exert H3K27M-dependent effects in pedHGG cells.

In addition, DIPG are very heterogenous tumors which leads to differential responses in tumors to therapeutic drugs depending on the tumor cell phenotype. Thus, two distinct cellular pedHGG phenotypes were examined: Gliospheres which resemble a more CSC-like phenotype and more differentiated DIPG cells grown as adherent monolayer cultures. Previous findings show that differentiated monolayer cells are more sensitive to treatment and grow faster than gliospheres (Meel et al. 2017).

4.1 The role of Curcumin in diffuse intrinsic pontine glioma

Curcumin is one of the most commonly used complementary treatment options for children with DIPG (El-Khouly et al. 2021). *In vitro*, Curcumin was shown to effectively inhibit tumor

cell proliferation in different tumor entities (Gersey et al. 2017). As expected, Curcumin reduced in the present study cell viability in a dose dependent manner in pedHGG cells. No statistically significant difference of cell viability between H3K27M-mutated DIPG-007 and control H3WT GBM-001 cells could be detected after treatment with Curcumin. In agreement with these results, previous studies in GBM cells obtained from adult patients observed a dose dependent reduction of cell viability after treatment with Curcumin (Gersey et al. 2017). Gersey et al. (2017) investigated different GBM cell lines and evaluated cell viability after treatment with Curcumin, reported IC₅₀ values ranging from 13.9 μ M to 39.5 μ M Curcumin in GBM stem-like cell lines and from 23.4 μ M to 30 μ M Curcumin for adherent cell lines. In comparison, the present study detected IC₅₀ values of approximately 14.8 μ M Curcumin for GBM-001 cells and 22.2 μ M Curcumin for DIPG-007 cells under stem-like conditions, thus, pedHGG cells responded similarly to Curcumin treatment as adult GBM cells. Our RNA-seq analysis of DIPG-007 cells uncovered that Curcumin particularly influences cell division and mitosis, which might explain the reduction of cell viability observed in MTT-cell viability assay. Future experiments may therefore focus on cell cycle assays to confirm the suggested impact of Curcumin on cell division and mitosis.

In addition, the impact of Curcumin on more differentiated non-CSC under adherent monolayer conditions was investigated in the present study. It was previously reported that non-CSC cells are more sensitive towards therapeutic treatments (Meel et al. 2017). Indeed, treatment with Curcumin led to stronger reduction of cell viability in non-CSC compared to CSC gliomaspheres independently of their H3-mutation status. Whether the observed differences in cell viability reduction between CSC and non-CSC depend on different gene expression could be investigated in future by performing RNA-seq of CSC and non-CSC after treatment with Curcumin.

The most commonly performed therapy for patients with DIPG consists of irradiation treatment in combination with TMZ chemotherapy (El-Khouly et al. 2019). To investigate if Curcumin sensitizes DIPG cells to irradiation and/or TMZ, DIPG-007 and GBM-001 gliomaspheres were subjected to TMZ with and without Curcumin followed by irradiation.

TMZ is an alkylating agent that adds a methyl group to pyrimidine and purine in DNA, which leads to DNA damage and therefore to cell cycle arrest and apoptosis. Both GBM-001 and DIPG-007 cells appeared to be widely resistant to treatment with TMZ alone. Adult GBM resistance towards TMZ was reported to depend on its methyl guanine methyl transferase (MGMT) DNA repair system (Karachi et al. 2018). Interestingly, a whole genome profiling of eleven DIPG patient samples revealed that MGMT was not expressed in any of the patient

derived tumor samples due to MGMT promoter DNA-methylation (Zarghooni et al. 2010). This leads to the conclusion that any potential chemotherapy resistance of DIPG may depend on other mechanisms different from the MGMT DNA repair system. Whether MGMT expression influences chemotherapy resistance in GBM-001 and DIPG-007 cells remains unknown but could be investigated using quantitative polymerase chain reaction to investigate MGMT mRNA expression and to analyze the DNA methylation status of the MGMT promoter as surrogate parameter.

A study performed by Gaspar et al. (2010) investigated the mechanism responsible for chemotherapy resistance in pedHGG. While the authors observed that chemotherapy resistance in some pedHGG cell lines depends on the MGMT DNA repair system, they also found an MGMT-independent escape mechanism: Gene expression analysis of chemotherapy-resistant pedHGG cells without MGMT expression compared to non-chemotherapy-resistant pedHGG cell lines revealed an increased expression of *HOX*-genes mediated by phosphoinositid-3 (PI3)-Kinase pathway signaling in chemotherapy-resistant pedHGG cells without MGMT expression (Gaspar et al. 2010). The role of *HOX*-genes in chemotherapy resistance is not clear but Costa et al. (2010) suggest that *HOXA9* overexpression inhibits apoptosis and increases cell proliferation, thereby minimizing the apoptotic effect of TMZ. However, the sensitizing effect of Curcumin combined with TMZ published for adult GBM (Yin et al. 2014) could only be reproduced for GBM-001 cells. While Curcumin sensitized GBM-001 cells to TMZ, this effect was not observed in DIPG-007 cells, suggesting that DIPG-007 cells may harbor specific mechanisms to evade the TMZ sensitizing effect of Curcumin. Interestingly, RNA-seq of DIPG-007 cells after treatment with Curcumin revealed a downregulation of *HOXA9* (data not shown) suggesting no impact via this pathway. Nevertheless, the role of *HOXA9* in GBM-001 cells sensitized towards TMZ by Curcumin still has to be investigated. It has been reported that inhibition of PI3-Kinase reverses the transcriptional activation of the *HOXA* cluster (Costa et al. 2010). Therefore, MTT-cell viability assays after inhibition of PI3-Kinase pathway and treatment with TMZ alone or in combination with Curcumin could be performed to investigate if *HOXA9* overexpression is responsible for the observed resistance of GBM-001 and DIPG-007 cells towards TMZ. In contrast, Yin et al. (2014) reported, that the generation of reactive oxygen species (ROS) and the inhibition of AKT/mTOR signaling pathway play an important role in the sensitizing effect of Curcumin towards TMZ in adult GBM cells. Whether the observed effect in the current study after treatment of pedHGG cells with Curcumin and TMZ depends on ROS and inhibition of AKT/mTOR signaling pathway has to be investigated too in future projects.

In contrast, another group observed an additive rather than a sensitizing effect in adult GBM cells after treatment with Curcumin and TMZ (Zanotto-Filho et al. 2015). They attributed this effect towards redundant effects of Curcumin and TMZ which led to autophagy. An inhibition of autophagy via knockdown of autophagy-related 7 homolog (*ATG7*) and addition of PI3-Kinase inhibitor 3-methyl-adenine led to increased cytotoxicity after treatment with Curcumin and TMZ (Zanotto-Filho et al. 2015). Interestingly, RNA-seq of DIPG-007 cells after treatment with Curcumin led to an upregulation of *ATG12* (data not shown), a protein mediated by *ATG7* and important for induction of autophagy (Fraiberg and Elazar 2020). This suggests that Curcumin treatment may indeed induce autophagy in DIPG-007 cells. To further investigate whether autophagy is responsible for an additive rather than sensitizing effect of Curcumin towards TMZ treatment in pedHGG cells could be investigated by using knockdown of *ATG7* and addition of PI3-Kinase inhibitor 3-methyl-adenine. Whether the observed stronger effect of Curcumin and TMZ in GBM-001 cells depends on reduced autophagy could be also examined by performing western blot analyses with antibodies against *ATG7*.

Curcumin in combination with TMZ further increased the anti-proliferative effect of TMZ in both pedHGG cell lines and appeared to have a synergistic effect on reduction of cell viability in GBM-001 cells. However, only two concentrations of Curcumin and TMZ were used in the present study. To determine if Curcumin and TMZ may indeed work synergistically in GBM-001 cells, dilution curves of TMZ and Curcumin alone and in combination should be performed, and different models could be used, such as the Loewe additivity or the Bliss model for synergy testing (Loewe 1953; Bliss 1956).

The present study showed that Curcumin combined with irradiation treatment further decreases the cell viability of pedHGG cells. In contrast to the previously described sensitizing effect of Curcumin towards irradiation treatment in adult GBM and rat glioma cells (Dhandapani et al. 2007; Meng et al. 2017), no sensitizing effect in pedHGG cells could be observed in the current study. The groups of Dhandapani et al. (2007) and Meng et al. (2017) attributed the sensitizing effect of Curcumin towards irradiation to the inhibition of DNA repair capacity of cells which leads to increased cell damage after combined treatment with Curcumin and irradiation. A downregulation of DNA repair enzyme gene activities, namely of MGMT, ERCC-1 and DNA-PK genes, was observed (Dhandapani et al. 2007). In the present study, RNA-seq revealed that none of these genes were differently expressed in DIPG-007 cells after treatment with Curcumin (data not shown), which might explain the absence of a sensitizing effect of Curcumin towards irradiation in pedHGG cells. Meng et al. (2017)

reported that an inhibition of the hedgehog signaling pathway is responsible for an increased therapeutic efficiency of irradiation after treatment with Curcumin. They observed a decrease of the positive sony hedgehog marker proteins SMO and Gli1 and an increase of Sufu, the suppressor protein of Gli1 (Meng et al. 2017). In the present study, a downregulation of *SMO* and *GLI1* but also a slight downregulation of *SUFU* were observed (data not shown). However, Meng et al. (2017) performed western blot analyses, while RNA-seq was performed in this study. Since no RNA-seq of GBM-001 cells after treatment with Curcumin was performed, it is not clear how Curcumin may influence sony hedgehog markers in GBM-001 cells. Further western blot analyses may be helpful in the future.

Further investigation of functional effects of Curcumin on pedHGG cells uncovered that the ability to form spheres was reduced in both DIPG-007 and GBM-001 cells after treatment with Curcumin, which is in line with the observed reduction of sphere formation published for adult GBM (Gersey et al. 2017). Indeed, Gersey et al. (2017) used lower concentrations of 2.5 μM Curcumin and longer incubation time of 14 days and observed a reduction of sphere formation of 60%, which is stronger than the effect observed in the present study. In agreement with the observed reduction of sphere formation, western blot analysis revealed a reduction of Oct4 levels in DIPG-007 cells after treatment with Curcumin. This is in line with a study from Tahmasebi Mirgani et al. (2014) who observed a downregulation of *OCT4A* and *OCT4B1* variants expression in adult GBM cells after treatment with 17.5 μM dendrosomal Curcumin. In contrast, RNA-seq of DIPG-007 cells after treatment with Curcumin did not show a downregulation of *OCT4A* or *OCT4B1* (data not shown), leading to the assumption that its decrease takes place at a posttranslational level.

Previous studies in our group have found that H3K27M-mutated pedHGG gliomaspheres express higher levels of different stem cell markers than H3WT pedHGG gliomaspheres. Amongst others, Oct4 was reduced in H3WT pedHGG cells suggesting that H3K27M-mutated pedHGG cell display a stronger stem-like potential than H3WT pedHGG cells (Wiese et al. 2020). In agreement with the study by Wiese et al. (2020), H3K27M-mutated DIPG-007 cells showed a 8.5-times higher sphere formation capability than control H3WT GBM-001 cells. Treatment with Curcumin reduced the number of DIPG-007 spheres stronger than the number of GBM-001 spheres. Therefore, the reduction of Oct4 after treatment with Curcumin might have a stronger effect in H3K27M-mutated DIPG-007 cells leading to a stronger reduction of spheres as compared to H3WT pedHGG cells. To further investigate this hypothesis, Oct4 levels in H3WT pedHGG cells after treatment with Curcumin could be examined. In addition, the expression of other stem cell markers like

Nestin and Sox2 after treatment with Curcumin could be investigated in future using western blot analyses.

The present study also showed that Curcumin reduced the colony formation ability in both DIPG-007 and GBM-001 cells which is in concordance with the observed reduction of colony formation ability by Curcumin in adult GBM (Gersey et al. 2017; Du et al. 2013). Gersey et al. (2017) used 2.5 μ M Curcumin on patient derived samples and longer incubation time of 14 days and observed a reduction of colony area to 5% while Du et al. (2013) used 10 to 40 μ M of Curcumin in human glioma cell lines over 12 days and observed a reduction of colonized area to about 25%. In the present study, colonized area of pedHGG was reduced to 28% after 4 or 7 days which is comparable to the reduction of colony formation observed by Du et al. (2013). Du et al. (2013) attributed this reduction to a reduced expression of *GLI1*, a protein associated with the hedgehog pathway. RNA-seq of DIPG-007 gliomaspheres after treatment with Curcumin revealed a downregulation of *GLI1* as well (data not shown). On the other hand, Gersey et al. (2017) attributed the observed changes to induction of ROS by Curcumin. Whether the downregulation of *GLI1* or an induction of ROS as proposed by Gersey et al. (2017) is responsible for the observed effect in the present setting remains to be investigated.

The reduction of colonized area was stronger in DIPG-007 than in GBM-001 cells. However, the difference was not as striking as seen for sphere formation and could be caused by the slower proliferation of GBM-001 cells. In addition to the self-renewing ability, colony formation assay investigates the proliferation ability of cells which was, as seen in the MTT-cell viability assay, not impaired differently between GBM-001 and DIPG-007 cells. Therefore, it could be hypothesized that the reduced colony formation of GBM-001 cells is due to an effect of Curcumin on proliferation rather than on the self-renewing ability of GBM-001 cells. This is supported by the observation that treatment with Curcumin led to a reduced number of large spheres and an increased number of small spheres in GBM-001 cells while the total number of spheres was only reduced after treatment with 10 μ M Curcumin. Furthermore, it was also described that Oct4 levels were reduced in both H3K27M-mutated DIPG-007 and H3WT GBM-001 cells when cultured under monolayer conditions but still expressed stronger in H3K27M-mutated DIPG-007 cells (Wiese et al. 2020). Thus, a reduction of Oct4 induced by Curcumin influences the colony formation ability of DIPG-007 cells stronger than of GBM-001 cells, but not as strong as their sphere formation ability. To confirm this hypothesis, western blot analysis of GBM-001 cells after treatment with Curcumin with antibodies against Oct4 could be performed in future.

85% of DIPG carry a H3K27M-mutation which is restricted to pediatric tumors (Gerges et al. 2013; Castel et al. 2015). The H3K27M-mutation changes the epigenetic landscape by a global reduction of H3K27me3 and a compensatory increase of H3K27ac, which plays an important role in tumorigenesis (Lewis et al. 2013).

Under physiological conditions, H3K27me3 formation is mediated by EZH2 (Margueron and Reinberg 2011). A Curcumin induced reduction of *EZH2* expression was observed in pancreatic ductal adenocarcinoma cells and lung cancer (Yoshida et al. 2017; Wu et al. 2016). In this study, Curcumin had no statistically significant impact on H3K27me3 level in H3K27M-mutated DIPG-007 or control H3WT GBM-001 cells. Interestingly, RNA-seq of DIPG-007 cells after treatment with Curcumin revealed a downregulation of *EZH2* (data not shown) which is in line with previous studies (Yoshida et al. 2017; Wu et al. 2016). However, reduction of *EZH2* expression does not seem to influence the H3K27me3 level in DIPG-007 cells which is in line with a study conducted by Keane et al. (2021). They performed a knockdown of *EZH2* in DIPG cells but did not observe any changes in H3K27me3 levels after 72 h and proposed a low turnover of H3K27me3 as an explanation (Keane et al. 2021).

HAT CBP activity generates H3K27ac under physiological conditions (Jin et al. 2011). Azad et al. (2013) observed a reduction of H3K27ac and H4K8ac in yeast after treatment with Curcumin and proposed that iron chelating properties of Curcumin are responsible for this effect. Unlike Azad et al. (2013) others suggested inhibition of HAT activity of CBP/p300 as a potential mechanism leading to depletion of H3K27ac by Curcumin in neuroblastoma cells (Lu et al. 2014). The ability of Curcumin to inhibit the HAT activity of CBP/p300 was reported by other groups as well (Balasubramanyam et al. 2004).

Curcumin reduced H3K27ac and H4K8ac level in DIPG-007 cells which is in line with previous studies (Azad et al. 2013; Lu et al. 2014). However, Azad et al. (2013) used very high concentrations of Curcumin (400 μ M), shorter incubation times (1 to 3 h) and observed comparable levels of H3K27ac reduction. In addition to reduction of H3K27ac, decreased H4K8ac levels were also observed in the present study. Since H4K8ac is mediated by CBP/p300 (Henry et al. 2013), these results also hint towards an inhibition of CBP/p300 by Curcumin in DIPG-007 cells.

Interestingly, reduction of H3K27ac and H4K8ac levels after treatment with Curcumin in control H3WT GBM-001 cells was not as strong as in H3K27M-mutated DIPG-007 cells. The H3K27M-mutation usually leads to an increase of H3K27ac levels compared to H3WT cells (Lewis et al. 2013). Therefore, an inhibition of CBP/p300 might have a stronger impact on H3K27ac levels in H3K27M-mutated DIPG-007 cells than in H3WT GBM-001 cells. In

line with this hypothesis, Yan et al. (2017) reported a reduction of induced H3K9-hyperacetylation after alcohol exposure by Curcumin in cardiac cells of mice while Curcumin did not reduce physiological H3K9ac levels without prior induction of hyperacetylation. If elevated H3K27ac levels indeed are responsible for the stronger reduction of H3K27ac in DIPG-007 cells remains to be investigated.

Acetylation of H4 is presumed to play an important role in double strand DNA repair and replication origins (Gursoy-Yuzugullu et al. 2017; Unnikrishnan et al. 2010). Treatment of DIPG-007 cells with Curcumin resulted in H4K8ac depletion, an upregulation of genes associated with apoptosis, and a downregulation of genes associated with cell cycle progression, pointing to a general function of Curcumin to inhibit cell growth and mitosis. These results explain the inhibitory effects of Curcumin on cell viability and clonogenicity. Western blot analysis revealed a downregulation of H3K27ac and H4K8ac in DIPG-007 cells after treatment with Curcumin, which could be responsible for the observed changes of gene expression. To analyze if the differently transcribed genes identified by RNA-seq are associated with H3K27ac or H4K8ac, chromatin immunoprecipitation sequencing with antibodies against H3K27ac and H4K8ac could be performed.

Furthermore, Curcumin induced an increase of apoptosis marker Cleaved Caspase 3 levels in DIPG-007 cells which is in line with previous studies that describe an upregulation of Cleaved Caspase 3 after treatment with Curcumin in adult GBM cells (Yeh et al. 2015). However, this effect was not visible in the control GBM-001 cells. RNA-seq of DIPG-007 cells revealed an upregulation of apoptosis and an induction of cell cycle arrest, which explains the inhibitory effects of Curcumin on cell viability and proliferation. However, the mechanisms behind the observed effects of Curcumin in GBM-001 cells are not as clear and could be investigated using polymerase chain reaction on important target genes identified by RNA-seq in DIPG-007 cells.

An analysis of the differently expressed genes in DIPG-007 cells after treatment with Curcumin with the KEGG pathways database revealed that Curcumin downregulates many genes which are involved in cell cycle progression. These results are in line with previous studies which observed an induction of G2/M arrest by Curcumin in adult GBM cells (Cheng et al. 2016; Wang et al. 2015). To evaluate the extend of the observed RNA expression changes of genes associated with cell cycle progression, flow cytometry with propidium iodide staining could be performed.

For the present discussion, it may also be of some importance that Curcumin had been described to belong to the group of pan-assay interference compounds (PAINS). PAINS

interfere with certain assay readouts as a kind of artefact than through specific compound/target interactions (Nelson et al. 2017). However, the present study did not investigate specific compound/target interactions but focused on more general effects of Curcumin e.g. inhibition of proliferation and induction of cell death. No specific inconsistencies in regards to assay results were observed. Especially RNA-seq revealed an upregulation of apoptosis and an induction of cell cycle arrest which cannot solely be explained through assay readout interference. However, further investigations should consider chemical properties of Curcumin, and counterscreens should be additionally performed to rule out any potential assay interference.

4.2 The role of Boswellic acids in diffuse intrinsic pontine glioma

Besides Curcumin, parents of children with DIPG often use BA-supplements as complementary treatment option, which contain the three BA α -BA, β -BA and AKBA (El-Khouly et al. 2021).

It was previously reported that BA reduce cell viability in different cancer cells amongst others in adult GBM cells (Schneider and Weller 2016). Investigation of the effect of α -BA, β -BA, and AKBA in pedHGG cells showed that all three BA reduced cell viability with dosages higher than 13.34 μ M. Schneider and Weller (2016) used long-term adult GBM cell lines (LTC) as well as primary patient-derived glioma initiating cells (GIC) and applied BA concentrations ranging from 1.95 μ M to 220 μ M for 72 h. While cell viability of LTC was already decreased after treatment with concentrations of 1.95 μ M to 10 μ M BA, cell viability of GIC was only decreased after treatment with concentrations of 10 μ M to 20 μ M BA (Schneider and Weller 2016) which is in line with the observed effect in the present study.

However, an increase in cell viability after treatment of DIPG-007 spheroid cells with lower dosages of α -BA and β -BA was observed hinting towards a potential tumor propagating effect of low dosages of α -BA and β -BA. In contrast, treatment with AKBA decreased cell viability of both DIPG-007 and GBM-001 cells in a dose dependent manner. Comparable levels of AKBA reduced cell viability more efficiently than α -BA and β -BA. These findings are in line with previous studies which reported AKBA as the most potent BA (Schneider and Weller 2016).

Apart from the slight increase of cell viability of DIPG-007 spheroid cells after treatment with low dosages of α -BA or β -BA, no significant different impact on cell viability between DIPG-007 and GBM-001 cells was observed. Since treatment with AKBA did not lead to different effects on cell viability in H3K27M-mutated DIPG-007 and H3WT GBM-001 it appears that

AKBA may influence cell viability of pedHGG cells independently of their H3-mutation status. In addition, neither western blot analysis nor RNA-seq revealed relevant changes in protein or gene expression after treatment with BA, indicating more general and less H3K27M-specific BA-mediated effects.

It was previously shown that non-CSC are more sensitive to drug treatment (Meel et al. 2017) and therefore it was expected that DIPG-007 and GBM-001 non-CSC grown as adherent monolayer cells under differentiating conditions may show a stronger response to treatment with BA. Interestingly, a stronger effect between non-CSC and CSC was only observed in GBM-001 cells after treatment with α -BA. No difference in cell viability was observed in DIPG-007 CSC and non-CSC. Moreover, treatment with AKBA showed no difference of cell viability between CSC and non-CSC in both pedHGG cell lines. This is in contrast to the study conducted by Schneider and Weller (2016) who used LTC, grown under adherent monolayer conditions with 10% FCS, and GIC, grown under spheroid conditions. Here, LTC were more sensitive towards treatment with all three BA (Schneider and Weller 2016). In the present study, the two pedHGG cell lines were cultured under different conditions which may explain the observed differences.

The H3K27M-mutation influences the epigenetic landscape by reduction of H3K27 trimethylation and parallel increase of acetylation (Lewis et al. 2013; Bender et al. 2013). The association of H3K27me₃ with gene repression may support its function as a potential tumor driver (Castel et al. 2018). AKBA was observed to induce epigenetic changes via modulation of DNA methylation in colorectal cancer cells (Shen et al. 2012). However, no influence of BA on histone modifications has been reported this far. Since treatment with BA reduced cell viability of DIPG-007 cells, the influence of BA on epigenetic marks, namely H3K27me₃, H3K27ac, and H4K8ac levels, were investigated. In the present study, western blot analyses only showed a slight decrease of H3K27ac after treatment with 20 μ M α -BA and a slight decrease of H4K8ac after treatment with 20 μ M AKBA but no changes in H3K27me₃-levels. However, the western blots were only performed twice with reduced overall quality. To investigate if BA have any significant impact on histone modifications, western blot analyses would have to be repeated and/or even performed with other pedHGG cell lines. Nevertheless, so far the present results suggest that the observed anti-tumor effects of BA might not be based on changes in the epigenetic landscape which is also supported by the observation that treatment with AKBA led to no differently transcribed genes in DIPG-007 cells.

Since it was reported that BA reduce clonogenicity in adult GBM (Schneider and Weller 2016) and differentiated monolayer cells are more sensitive towards treatment (Meel et al. 2017) the clonogenicity of H3K27M-mutated DIPG-007 and H3WT GBM-001 cells after treatment with BA has been examined. DIPG-007 cells displayed a dose dependent reduction of colony area under differentiated monolayer conditions after treatment with BA, which is in line with the study by Schneider and Weller (2016). However, colony formation ability of GBM-001 cells was not reduced after treatment with BA. Treatment with 20 μ M α -BA even increased the ability of GBM-001 cells to form colonies. As colony formation assay usually represents self-renewal ability and proliferation ability these results may be on first sight in contrast to the observations of the MTT-cell viability assay showing no differences of cell viability between DIPG-007 and GBM-001 adherent monolayer cells after treatment with BA. But since GBM-001 cells proliferate slower than DIPG-007 cells, the different effects of BA on clonogenicity in pedHGG cells might still be due to an effect on proliferation rather than on self-renewal ability. This is supported by the results from sphere formation assays which showed no reduction but rather a slight increase of sphere formation ability in DIPG-007 and GBM-001 cells after treatment with BA which hints towards a beneficial effect of BA on self-renewal ability.

Whereas a reduction of cell viability of both DIPG-007 and GBM-001 spheroid cells at dosages higher than 13.34 μ M of BA was observed, the total number of spheres was not reduced after treatment with 20 μ M BA. Treatment with β -BA even led to a slight increase of the number of spheres. This may suggest that BA do not reduce self-renewal ability and stemness of pedHGG cells.

However, an increase of small spheres and a decrease of large spheres of DIPG-007 cells was detected indicating a slowing of cell proliferation. This is in line with the observations from the MTT-cell viability assay, where a reduction of cell viability could be observed. In contrast, Schneider and Weller (2016) observed a reduction of sphere formation in adult GIC after treatment with 19.5 μ M AKBA, 22 μ M α -BA, and 22 μ M β -BA. However, the mechanism behind the observed effects was not illuminated but hypothesized to depend on acute cytotoxicity (Schneider and Weller 2016). In the present study, RNA-seq revealed no differently expressed genes in DIPG-007 cells after treatment with AKBA, leading to the assumption that BA might not influence transcription in pedHGG cells. These results suggest that the inhibitory effect of BA is due to cytotoxicity caused by high dosages.

Interestingly, Li et al. (2018) published that in adult glioblastoma AKBA influenced transcription of genes associated with cell cycle arrest and DNA replication. In the present

study, no differently transcribed genes in DIPG-007 cells after treatment with AKBA could be detected, even though dosage and incubation time were the same as in the study published by Li et al. (2018). However, another study, published by Schneider and Weller (2016) investigated the effect of AKBA on glioma LTC lines and primary patient derived GIC and found that treatment with AKBA induced cell cycle arrest in LTC lines while even 10-fold higher AKBA doses induced only a still weak effect. Interestingly, in the study conducted by Schneider and Weller (2016), LTC were cultured with 10% FCS, while GIC were cultured without FCS, Li et al. (2018) also added 10% fetal bovine serum to the medium. Fetal calf serum or fetal bovine serum causes cells to grow as adherent cells under differentiating conditions. This suggests that GIC, cultured under more CSC-like conditions, were more resistant towards AKBA treatment (Schneider and Weller 2016). Since LTC in the study by Schneider and Weller (2016) and adult GBM cells in the study performed by Li et al. (2018) were cultured under more differentiated conditions and were more sensitive towards AKBA treatment, all these findings may hint towards a phenotype-dependent effect of AKBA. In the present study, colony formation assay revealed a reduction of clonogenicity of DIPG-007 cells after treatment with AKBA while sphere formation ability of DIPG-007 cells was not impaired after treatment with AKBA. However, RNA-seq was performed with cells cultured under spheroid conditions which could explain the difference between this study and the study performed by Li et al. (2018) or Schneider and Weller (2016). To confirm this hypothesis, RNA-seq with cells cultured under adherent monolayer conditions after treatment with BA could be performed.

As already reported for adult glioblastoma (Conti et al. 2018; Schneider and Weller 2016), a positive effect of BA was observed in combination with the chemotherapeutic TMZ. Such an effect was only observed in H3WT GBM-001 but not in H3K27M-mutated DIPG-007 cells. TMZ combined with BA led to a stronger reduction of cell viability in GBM-001 cells than in DIPG-007 cells, leading to the assumption, that DIPG-007 cells harbor specific mechanisms to evade a sensitizing effect towards TMZ.

BA appeared to mediate synergistic effects with TMZ in GBM-001 cells. However, to proof if BA and TMZ work synergistically, the effect on cell viability of more than two concentrations of BA and TMZ alone and in combination have to be investigated for application of synergy models, such as the Loewe additivity or the Bliss models (Loewe 1953; Bliss 1956).

Conti et al. (2018) reported that AKBA influences irradiation treatment in adult GBM cells. They observed an additive effect of low dosages of AKBA (10 μ M, 20 μ M and 30 μ M) in combination with irradiation and a synergistic effect of high dosages of AKBA (40 μ M).

Investigation of the underlying mechanisms revealed a decreased expression of Tp53 and the anti-apoptotic protein Bcl-2 as well as inhibition of NF- κ B signaling which is associated with radiotherapy resistance by increase (Conti et al. 2018). In the present study, 10 μ M and 20 μ M of AKBA, α -BA, and β -BA were used, and α -BA and AKBA increased the cell viability reducing effect of irradiation. But unlike Conti et al. (2018), RNA-seq of DIPG-007 cells after treatment with AKBA revealed no differentially expressed genes. If treatment of DIPG-007 and GBM-001 cells with AKBA influences Tp53, Bcl-2 or NF- κ B signaling on a posttranslational level remains to be investigated in future.

4.3 Are Curcumin and Boswellic acids potential complementary treatment options?

The aim of the present study was to investigate if Curcumin and BA could serve as potential complementary treatment options for children with DIPG. It was found that Curcumin and BA induce cell viability reducing effects in DIPG-007 and GBM-001 cells. However, while Curcumin influenced epigenetic marks and gene expression, BA influenced neither one and even showed some tumor promoting properties. This suggests that Curcumin may exhibit a higher potential as complementary therapy option for children with DIPG.

BA have been used in a clinical trial to reduce cerebral edema after irradiation (Kirste et al. 2011). Cerebral edema and inflammatory processes are the main morbidity reason in brain tumor patients. Usually, cerebral edema is treated with steroids, primarily dexamethasone, which displays severe adverse effects and might even promote tumor growth. The study by Kirste et al. (2011) proposed BA as an alternative treatment option for cerebral edema treatment with decreased adverse effects in comparison with dexamethasone treatment. This study was performed only in a small group of adult patients. To confirm the effect of BA in children, further studies should be conducted. However, the results of the present study showed, that BA do not negatively interact with radiochemotherapy. Thus, BA may be indeed a good replacement for dexamethasone as anti-edema treatment if efficacy appears similar.

BA supplements often consist of different BA derivatives in low dosages. Since an increase of cell viability and sphere formation ability after treatment with α -BA and β -BA but not AKBA was observed, the usage of mixed BA supplements must be questioned. If α -BA and β -BA indeed increase tumor proliferation at low dosages, their application can harm DIPG patients. Parents or caretakers of patients with DIPG often apply CAM to the patients without the knowledge of their physician (El-Khouly et al. 2021). Especially if compounds like BA might harm DIPG patients, physicians should be aware of the usage of CAM.

Curcumin exhibited potential as a therapeutic agent for treatment of DIPG patients. The H3K27M-mutation and its subsequent changes of the epigenetic landscape play an important role in tumorigenesis in DIPG (Xu et al. 2017; Schwartzentruher et al. 2012). Thus, the ability of Curcumin to reduce H3K27ac, as seen in the present study may be relevant for its therapeutic application in DIPG.

It has been reported that Curcumin exhibits a low oral bioavailability due to its poor water solubility and therefore poor absorption, its fast metabolism, and its fast elimination (Anand et al. 2007). Various clinical studies detected plasma levels of Curcumin in the nanomolar scope even after application of relatively high oral dosages (Dei Cas and Ghidoni 2019). Since the health benefiting properties of Curcumin have been proposed for a long time, several strategies to overcome this obstacle are under investigation. One approach is to combine Curcumin with other substrates for example piperine, a derivate of black pepper, to increase its bioavailability. Even though measured plasma levels of Curcumin after combination with piperine were higher than without, the maximum concentration in plasma was only 0.48 μM Curcumin (Volak et al. 2013). Another attempt is to dissolve Curcumin in polyethylene glycols to create an emulsion for better solubility. A study in mice achieved Curcumin plasma levels of 12.6 μM after oral administration of 1800mg/kg of Curcumin emulsion (Zhongfa et al. 2012). The safety for humans and long-term adverse effects of Curcumin emulsion remain to be investigated. Another approach to overcome the poor bioavailability is to enhance the water solubility of Curcumin by adding hydrophilic groups (Theppawong et al. 2019). To reach the tumor, Curcumin has to pass the BBB. Hydrophobic and therefore lipophilic agents can cross the BBB without help of carrier proteins. While Curcumin, a highly lipophilic agent, was reported to be able to cross the BBB (Perry et al. 2010) this has to be investigated for modified Curcumin derivates. Furthermore, it has to be investigated if chemically changed Curcuminoids still display the same anti-tumorigenic functions as Curcumin.

Critics purport that the increase of plasma levels of Curcumin does not only increase its effectiveness against disease but might also lead to increased toxicity (Burgos-Morón et al. 2010). This must be carefully considered since Curcumin does not only exhibit health benefitting properties. It was reported that Curcumin has cytotoxic effects on human kidney cells and a murine macrophage cell line with IC_{50} values of 15.2 μM and 31 μM (Nelson et al. 2017). However, an *in vivo* study with Curcumin reported a survival benefit of mice with glioblastoma even at high plasma levels of Curcumin (Wang et al. 2017). Considering that the median survival of DIPG patients is 11 months (Hoffman et al. 2018), even an improvement of survival for a few months would represent a success in therapy, and long-term adverse

effects might not be as important as in other diseases. Still, animal experiments should be performed first, and clinical trials with high plasma levels of Curcumin must be monitored closely for adverse effects; potential benefits have to be carefully weighed up against side effects.

In summary, this study shows that BA reduce cell viability of pedHGG cells and positively influence standard treatment consisting of irradiation and TMZ but since they do not influence histone modifications or RNA-expression, this effect is hypothesized to depend on acute cytotoxicity. Furthermore, low dosages of α -BA and β -BA even seemed to have tumor promoting effects. On the other hand, Curcumin reduced cell viability in a dose dependent manner and positively influenced standard treatment. In addition, Curcumin also influenced relevant histone modifications, induced cell cycle arrest and apoptosis and reduced clonogenicity and stemness.

Overall, the present study showed that Curcumin appears to be a promising complementary treatment option for children with DIPG and is worth further investigation while the use of BA as complementary treatment for children with DIPG especially in low dosages should be considered critically.

5 Conclusion

Diffuse intrinsic pontine glioma is a rare but lethal brain tumor with a median survival of eleven months after diagnosis. There has been no significant improvement in survival over the past 50 and more years despite intensive research. Therefore, parents of affected children may often use alternative complementary treatment options such as Curcumin and Boswellic acids. However, the data evaluating the effect of these compounds in diffuse intrinsic pontine glioma is limited. Therefore, the aim of the present study was to evaluate the therapeutic potential of Curcumin and Boswellic acids in an *in vitro* model of diffuse intrinsic pontine glioma.

Curcumin reduced cell viability of pediatric high grade glioma cells in a dose dependent manner. However, no statistically significant differences in reduction of cell viability between DIPG-007 and GBM-001 cells could be detected. Furthermore, Curcumin reduced stemness and clonogenicity of pediatric high grade glioma cells and reduced levels of the stemness marker Oct4 in DIPG-007 cells. The H3K27M-mutation influences the epigenetic landscape by increasing H3K27-acetylation and reducing H3K27-trimethylation and promotes tumor growth. Treatment with Curcumin influenced the epigenetic landscape by reducing H3K27-acetylation and H4K8-acetylation hinting towards an inhibition of the histone acetyl transferase activity of the cyclic adenosine monophosphate response element binding protein binding protein by Curcumin. Remarkably, this effect was stronger in H3K27M-mutated DIPG-007 cells than in H3-wildtype GBM-001 cells suggesting that Curcumin has a stronger influence on high acetylation levels. Moreover, RNA-sequencing of DIPG-007 cells after treatment with Curcumin revealed an upregulation of genes associated with apoptosis and cell cycle arrest, leading to the assumption that Curcumin inhibits cell proliferation and mitosis. When combined with standard therapy consisting of irradiation and temozolomide Curcumin further increased their proliferation/cell viability inhibiting effect and even sensitized GBM-001 cells towards temozolomide.

The three Boswellic acids derivatives α -Boswellic Acid, β -Boswellic Acid, and 3-O-Acetyl-11-Keto- β -Boswellic Acid decreased cell viability in a dosage higher than 20 μ M with no statistically significant differences between DIPG-007 and GBM-001 cells. However, α -Boswellic Acid and β -Boswellic Acid slightly increased cell viability in low dosages. In addition, sphere formation ability in both cell lines and colony formation ability in GBM-001 cells was not reduced after treatment with Boswellic acids. Only colony formation ability of DIPG-007 cells was reduced after treatment with Boswellic acids. Moreover, Boswellic acids

did not influence the epigenetic marks H3K27-trimethylation, H3K27-acetylation, and H4K8-acetylation and 3-O-Acetyl-11-Keto- β -Boswellic Acid, the most potent Boswellic acid, did not influence gene expression in DIPG-007 cells at all, hinting towards a cytotoxic effect of Boswellic acids caused by high dosages. When combined with standard therapy, Boswellic acids further increased their cell viability reducing effect and even sensitized GBM-001 cells to temozolomide.

In conclusion, Curcumin exhibits greater potential as complementary treatment option for children with diffuse intrinsic pontine glioma while the application of Boswellic acids as complementary treatment for children with diffuse intrinsic pontine glioma especially in low dosages should be considered critically.

6 References

- Ahmed HH, Abd-Rabou AA, Hassan AZ, Kotob SE (2015): Phytochemical Analysis and Anti-cancer Investigation of *Boswellia serrata* Bioactive Constituents In Vitro. *Asian Pac J Cancer Prev* 16, 7179–7188
- Anand P, Kunnumakkara AB, Newman RA, Aggarwal BB (2007): Bioavailability of curcumin: problems and promises. *Mol Pharm* 4, 807–818
- Azad GK, Singh V, Golla U, Tomar RS (2013): Depletion of Cellular Iron by Curcumin Leads to Alteration in Histone Acetylation and Degradation of Sml1p in *Saccharomyces cerevisiae*. *PLoS One* 8, e59003
- Balasubramanyam K, Varier RA, Altaf M, Swaminathan V, Siddappa NB, Ranga U, Kundu TK (2004): Curcumin, a novel p300/CREB-binding protein-specific inhibitor of acetyltransferase, represses the acetylation of histone/nonhistone proteins and histone acetyltransferase-dependent chromatin transcription. *J Biol Chem* 279, 51163–51171
- Ballester LY, Wang Z, Shandilya S, Miettinen M, Burger PC, Eberhart CG, Rodriguez FJ, Raabe E, Nazarian J, Warren K et al. (2013): Morphologic characteristics and immunohistochemical profile of diffuse intrinsic pontine gliomas. *Am J Surg Pathol* 37, 1357–1364
- Beghelli D, Isani G, Roncada P, Andreani G, Bistoni O, Bertocchi M, Lupidi G, Alunno A (2017): Antioxidant and Ex Vivo Immune System Regulatory Properties of *Boswellia serrata* Extracts. *Oxid Med Cell Longev* 2017, 7468064
- Bender S, Tang Y, Lindroth AM, Hovestadt V, Jones DTW, Kool M, Zapatka M, Northcott PA, Sturm D, Wang W et al. (2013): Reduced H3K27me3 and DNA Hypomethylation Are Major Drivers of Gene Expression in K27M Mutant Pediatric High-Grade Gliomas. *Cancer Cell* 24, 660–672
- Bird A (2007): Perceptions of epigenetics. *Nature* 447, 396–398
- Bliss CI (1956): The calculation of microbial assays. *Bacteriological Reviews* 20, 243–258
- Braunstein S, Raleigh D, Bindra R, Mueller S, Haas-Kogan D (2017): Pediatric high-grade glioma: current molecular landscape and therapeutic approaches. *J Neurooncol* 134, 541–549
- Burgos-Morón E, Calderón-Montaña JM, Salvador J, Robles A, López-Lázaro M (2010): The dark side of curcumin. *International Journal of Cancer* 126, 1771–1775
- Castel D, Philippe C, Calmon R, Le Dret L, Truffaux N, Boddaert N, Pagès M, Taylor KR, Saulnier P, Lacroix L et al. (2015): Histone H3F3A and HIST1H3B K27M mutations define two subgroups of diffuse intrinsic pontine gliomas with different prognosis and phenotypes. *Acta Neuropathol* 130, 815–827

- Castel D, Philippe C, Kergrohen T, Sill M, Merlevede J, Barret E, Puget S, Sainte-Rose C, Kramm CM, Jones C et al. (2018): Transcriptomic and epigenetic profiling of 'diffuse midline gliomas, H3 K27M-mutant' discriminate two subgroups based on the type of histone H3 mutated and not supratentorial or infratentorial location. *Acta Neuropathol Commun* 6, 117
- Cheng C, Jioa JT, Qian Y, Guo XY, Huang J, Dai MC, Zhang L, Ding XP, Zong D, Shao JF (2016): Curcumin induces G2/M arrest and triggers apoptosis via FoxO1 signaling in U87 human glioma cells. *Mol Med Rep* 13, 3763–3770
- Cohen I, Poreba E, Kamieniarz K, Schneider R (2011): Histone Modifiers in Cancer: Friends or Foes? *Genes Cancer* 2, 631–647
- Conti S, Vexler A, Edry-Botzer L, Kalich-Philosoph L, Corn BW, Shtraus N, Meir Y, Hagoel L, Shtabsky A, Marmor S et al. (2018): Combined acetyl-11-keto- β -boswellic acid and radiation treatment inhibited glioblastoma tumor cells. *PLoS One* 13, e0198627
- Costa BM, Smith JS, Chen Y, Chen J, Phillips HS, Aldape KD, Zardo G, Nigro J, James CD, Fridlyand J et al. (2010): Reversing HOXA9 oncogene activation by PI3K inhibition: epigenetic mechanism and prognostic significance in human glioblastoma. *Cancer Res* 70, 453–462
- Dei Cas M, Ghidoni R (2019): Dietary Curcumin: Correlation between Bioavailability and Health Potential. *Nutrients* 11, 2147
- Dhandapani KM, Mahesh VB, Brann DW (2007): Curcumin suppresses growth and chemoresistance of human glioblastoma cells via AP-1 and NFkappaB transcription factors. *J Neurochem* 102, 522–538
- Du WZ, Feng Y, Wang XF, Piao XY, Cui YQ, Chen LC, Lei XH, Sun X, Liu X, Wang HB et al. (2013): Curcumin suppresses malignant glioma cells growth and induces apoptosis by inhibition of SHH/GLI1 signaling pathway in vitro and vivo. *CNS Neurosci Ther* 19, 926–936
- Du Z, Liu Z, Ning Z, Liu Y, Song Z, Wang C, Lu A (2015): Prospects of boswellic acids as potential pharmaceuticals. *Planta Med* 81, 259–271
- El-Khouly FE, Adil SM, Wiese M, Hulleman E, Hendrikse NH, Kaspers GJL, Kramm CM, van Veldhuijzen Zanten SEM, van Vuurden DG (2021): Complementary and alternative medicine in children with diffuse intrinsic pontine glioma-A SIOPE DIPG Network and Registry study. *Pediatr Blood Cancer* 68, e29061
- El-Khouly FE, van Veldhuijzen Zanten SEM, Santa-Maria Lopez V, Hendrikse NH, Kaspers GJL, Loizos G, Sumerauer D, Nysom K, Pruunsild K, Pentikainen V et al. (2019): Diagnostics and treatment of diffuse intrinsic pontine glioma: where do we stand? *J Neurooncol* 145, 177–184
- Erdmann F, Kaatsch P, Grabow D, Spix C: German Childhood Cancer Registry - Annual Report 2019: 1980-2018; Verlag Kirchheim + Co GmbH, Mainz 2020

- Fangusaro J (2012): Pediatric high grade glioma: a review and update on tumor clinical characteristics and biology. *Front Oncol* 2, 105
- Filbin MG, Suva ML (2016): Gliomas Genomics and Epigenomics: Arriving at the Start and Knowing It for the First Time. *Annu Rev Pathol* 11, 497–521
- Fraiberg M, Elazar Z (2020): Genetic defects of autophagy linked to disease. *Prog Mol Biol Transl Sci* 172, 293–323
- Frank MB, Yang Q, Osban J, Azzarello JT, Saban MR, Saban R, Ashley RA, Welter JC, Fung KM, Lin HK (2009): Frankincense oil derived from *Boswellia carteri* induces tumor cell specific cytotoxicity. *BMC Complement Altern Med* 9, 6
- Gaspar N, Marshall L, Perryman L, Bax DA, Little SE, Viana-Pereira M, Sharp SY, Vassal G, Pearson ADJ, Reis RM et al. (2010): MGMT-independent temozolomide resistance in pediatric glioblastoma cells associated with a PI3-kinase-mediated HOX/stem cell gene signature. *Cancer Res* 70, 9243–9252
- Gerbeth K, Husch J, Fricker G, Werz O, Schubert-Zsilavec M, Abdel-Tawab M (2013): In vitro metabolism, permeation, and brain availability of six major boswellic acids from *Boswellia serrata* gum resins. *Fitoterapia* 84, 99–106
- Gerges N, Fontebasso AM, Albrecht S, Faury D, Jabado N (2013): Pediatric high-grade astrocytomas: a distinct neuro-oncological paradigm. *Genome Med* 5, 66
- Gersey ZC, Rodriguez GA, Barbarite E, Sanchez A, Walters WM, Ohaeto KC, Komotar RJ, Graham RM (2017): Curcumin decreases malignant characteristics of glioblastoma stem cells via induction of reactive oxygen species. *BMC Cancer* 17, 99
- Griffith AA, Holmes W (2019): Fine Tuning: Effects of Post-Translational Modification on Hsp70 Chaperones. *Int J Mol Sci* 20, 4207
- Gupta SC, Patchva S, Aggarwal BB (2013): Therapeutic roles of curcumin: lessons learned from clinical trials. *AAPS J* 15, 195–218
- Gursoy-Yuzugullu O, Carman C, Price BD (2017): Spatially restricted loading of BRD2 at DNA double-strand breaks protects H4 acetylation domains and promotes DNA repair. *Sci Rep* 7, 12921
- Henry RA, Kuo YM, Andrews AJ (2013): Differences in specificity and selectivity between CBP and p300 acetylation of histone H3 and H3/H4. *Biochemistry* 52, 5746–5759
- Hesari A, Rezaei M, Rezaei M, Dashtiahangar M, Fathi M, Rad JG, Momeni F, Avan A, Ghasemi F (2018): Effect of curcumin on glioblastoma cells. *J Cell Physiol* 234, 10281–10288
- Hoffman LM, van Veldhuijzen Zanten SEM, Colditz N, Baugh J, Chaney B, Hoffmann M, Lane A, Fuller C, Miles L, Hawkins C et al. (2018): Clinical, Radiologic, Pathologic, and Molecular Characteristics of Long-Term Survivors of Diffuse Intrinsic Pontine Glioma (DIPG):

- A Collaborative Report From the International and European Society for Pediatric Oncology DIPG Registries. *J Clin Oncol* 36, 1963–1972
- Huang DW, Sherman BT, Lempicki RA (2009a): Bioinformatics enrichment tools: paths toward the comprehensive functional analysis of large gene lists. *Nucleic Acids Research* 37, 1–13
- Huang DW, Sherman BT, Lempicki RA (2009b): Systematic and integrative analysis of large gene lists using DAVID bioinformatics resources. *Nat Protoc* 4, 44–57
- Jin Q, Yu LR, Wang L, Zhang Z, Kasper LH, Lee JE, Wang C, Brindle PK, Dent SYR, Ge K (2011): Distinct roles of GCN5/PCAF-mediated H3K9ac and CBP/p300-mediated H3K18/27ac in nuclear receptor transactivation. *EMBO J* 30, 249–262
- Karachi A, Dastmalchi F, Mitchell DA, Rahman M (2018): Temozolomide for immunomodulation in the treatment of glioblastoma. *Neuro Oncol* 20, 1566–1572
- Keane L, Cheray M, Saidi D, Kirby C, Friess L, Gonzalez-Rodriguez P, Gerdes ME, Grabert K, McColl BW, Joseph B (2021): Inhibition of microglial EZH2 leads to anti-tumoral effects in pediatric diffuse midline gliomas. *Neuro-oncology Advances* 3, vdab096
- Kirste S, Treier M, Wehrle SJ, Becker G, Abdel-Tawab M, Gerbeth K, Hug MJ, Lubrich B, Grosu AL, Momm F (2011): *Boswellia serrata* acts on cerebral edema in patients irradiated for brain tumors: a prospective, randomized, placebo-controlled, double-blind pilot trial. *Cancer* 117, 3788–3795
- Korolev N, Lyubartsev AP, Nordenskiöld L (2018): A systematic analysis of nucleosome core particle and nucleosome-nucleosome stacking structure. *Sci Rep* 8, 1543
- Kouzarides T (2007): Chromatin modifications and their function. *Cell* 128, 693–705
- Kumar A, Chetia H, Sharma S, Kabiraj D, Talukdar NC, Bora U (2015): Curcumin Resource Database. *Database (Oxford)* 27, bav070
- Kuttan R, Bhanumathy P, Nirmala K, George MC (1985): Potential anticancer activity of turmeric (*Curcuma longa*). *Cancer Lett* 29, 197–202
- Lao CD, Ruffin MT, Normolle D, Heath DD, Murray SI, Bailey JM, Boggs ME, Crowell J, Rock CL, Brenner DE (2006): Dose escalation of a curcuminoid formulation. *BMC Complement Altern Med* 6, 10
- Lewis PW, Müller MM, Koletsky MS, Cordero F, Lin S, Banaszynski LA, Garcia BA, Muir TW, Becher OJ, Allis CD (2013): Inhibition of PRC2 Activity by a Gain-of-Function H3 Mutation Found in Pediatric Glioblastoma. *Science* 340, 857–861
- Li W, Liu J, Fu W, Zheng X, Ren L, Liu S, Wang J, Ji T, Du G (2018): 3-O-acetyl-11-keto- β -boswellic acid exerts anti-tumor effects in glioblastoma by arresting cell cycle at G2/M phase. *J Exp Clin Cancer Res* 37, 132

- Li Y, Tollefsbol TO (2016): Age-related epigenetic drift and phenotypic plasticity loss: implications in prevention of age-related human diseases. *Epigenomics* 8, 1637–1651
- Loewe S (1953): The problem of synergism and antagonism of combined drugs. *Arzneimittel-Forschung* 3, 285–290
- Louis DN, Perry A, Reifenberger G, Deimling A von, Figarella-Branger D, Cavenee WK, Ohgaki H, Wiestler OD, Kleihues P, Ellison DW (2016): The 2016 World Health Organization Classification of Tumors of the Central Nervous System: a summary. *Acta Neuropathol* 131, 803–820
- Louis DN, Perry A, Wesseling P, Brat DJ, Cree IA, Figarella-Branger D, Hawkins C, Ng HK, Pfister SM, Reifenberger G et al. (2021): The 2021 WHO Classification of Tumors of the Central Nervous System: a summary. *Neuro Oncol* 23, 1231–1251
- Lu X, Deng Y, Yu D, Cao H, Wang L, Liu L, Yu C, Zhang Y, Guo X, Yu G (2014): Histone acetyltransferase p300 mediates histone acetylation of PS1 and BACE1 in a cellular model of Alzheimer's disease. *PLoS One* 9, e103067
- Mackay A, Burford A, Carvalho D, Izquierdo E, Fazal-Salom J, Taylor KR, Bjerke L, Clarke M, Vinci M, Nandhabalan M et al. (2017): Integrated Molecular Meta-Analysis of 1,000 Pediatric High-Grade and Diffuse Intrinsic Pontine Glioma. *Cancer Cell* 32, 520-537.e5
- Mannino G, Occhipinti A, Maffei ME (2016): Quantitative Determination of 3-O-Acetyl-11-Keto- β Boswellic Acid (AKBA) and Other Boswellic Acids in *Boswellia sacra* Flueck (syn. *B. carteri* Birdw) and *Boswellia serrata* Roxb. *Molecules* 21, 1329
- Margueron R, Reinberg D (2011): The Polycomb Complex PRC2 and its Mark in Life. *Nature* 469, 343–349
- Meel MH, Sewing ACP, Waranecki P, Metselaar DS, Wedekind LE, Koster J, van Vuurden DG, Kaspers GJL, Hulleman E (2017): Culture methods of diffuse intrinsic pontine glioma cells determine response to targeted therapies. *Exp Cell Res* 360, 397–403
- Meng X, Cai J, Liu J, Han B, Gao F, Gao W, Zhang Y, Zhang J, Zhao Z, Jiang C (2017): Curcumin increases efficiency of γ -irradiation in gliomas by inhibiting Hedgehog signaling pathway. *Cell Cycle* 16, 1181–1192
- Mesev EV, Miller DS, Cannon RE (2017): Ceramide 1-Phosphate Increases P-Glycoprotein Transport Activity at the Blood-Brain Barrier via Prostaglandin E2 Signaling. *Mol Pharmacol* 91, 373–382
- Montgomery A, Adeyeni T, San K, Heuertz RM, Ezekiel UR (2016): Curcumin Sensitizes Silymarin to Exert Synergistic Anticancer Activity in Colon Cancer Cells. *J Cancer* 7, 1250–1257
- Nelson KM, Dahlin JL, Bisson J, Graham J, Pauli GF, Walters MA (2017): The Essential Medicinal Chemistry of Curcumin: Miniperspective. *J Med Chem* 60, 1620–1637
- Oppenheimer A (1937): Tumeric (Curcumin) in biliary diseases. *The Lancet* 229, 619–621

- Perry MC, Demeule M, Regina A, Moundjian R, Beliveau R (2010): Curcumin inhibits tumor growth and angiogenesis in glioblastoma xenografts. *Mol Nutr Food Res* 54, 1192–1201
- Prabhavathi K, Chandra USJ, Soanker R, Rani PU (2014): A randomized, double blind, placebo controlled, cross over study to evaluate the analgesic activity of *Boswellia serrata* in healthy volunteers using mechanical pain model. *Indian J Pharmacol* 46, 475–479
- Pulido-Moran M, Moreno-Fernandez J, Ramirez-Tortosa C, Ramirez-Tortosa M (2016): Curcumin and Health. *Molecules* 21, 264
- Ramakrishnan V (1997): Histone structure and the organization of the nucleosome. *Annu Rev Biophys Biomol Struct* 26, 83–112
- Roy NK, Parama D, Banik K, Bordoloi D, Devi AK, Thakur KK, Padmavathi G, Shakibaei M, Fan L, Sethi G et al. (2019): An Update on Pharmacological Potential of Boswellic Acids against Chronic Diseases. *Int J Mol Sci* 20, 4101
- Sadakerska-Chudy A, Filip M (2015): A Comprehensive View of the Epigenetic Landscape. Part II: Histone Post-translational Modification, Nucleosome Level, and Chromatin Regulation by ncRNAs. *Neurotox Res* 27, 172–197
- Samarth G, Suwan K, Al-Bahrani M, Asavarut P, Hajitou A (2018): PDTM-32. The Novel Therapeutic Curcumin Enhances Targeted Bacteriophage Mediated in-vitro Cell Death in Primary Human Diffuse Intrinsic Pontine Glioma. *Neuro Oncol* 20, vi210
- Schneider H, Weller M (2016): Boswellic acid activity against glioblastoma stem-like cells. *Oncol Lett* 11, 4187–4192
- Schwartzentruber J, Korshunov A, Liu XY, Jones DTW, Pfaff E, Jacob K, Sturm D, Fontebasso AM, Quang DAK, Tonjes M et al. (2012): Driver mutations in histone H3.3 and chromatin remodelling genes in paediatric glioblastoma. *Nature* 482, 226–231
- Sengupta K, Alluri KV, Satish AR, Mishra S, Golakoti T, Sarma KV, Dey D, Raychaudhuri SP (2008): A double blind, randomized, placebo controlled study of the efficacy and safety of 5-Loxin for treatment of osteoarthritis of the knee. *Arthritis Res Ther* 10, R85
- Shanmugam MK, Rane G, Kanchi MM, Arfuso F, Chinnathambi A, Zayed ME, Alharbi SA, Tan BKH, Kumar AP, Sethi G (2015): The Multifaceted Role of Curcumin in Cancer Prevention and Treatment. *Molecules* 20, 2728–2769
- Shen Y, Takahashi M, Byun HM, Link A, Sharma N, Balaguer F, Leung HCE, Boland CR, Goel A (2012): Boswellic acid induces epigenetic alterations by modulating DNA methylation in colorectal cancer cells. *Cancer Biol Ther* 13, 542–552
- Shin HJ, Lee S, Jung HJ (2019): A curcumin derivative hydrazinobenzoylcurcumin suppresses stem-like features of glioblastoma cells by targeting Ca(2+) /calmodulin-dependent protein kinase II. *J Cell Biochem* 120, 6741–6752

- Tahmasebi Mirgani M, Isacchi B, Sadeghizadeh M, Marra F, Bilia AR, Mowla SJ, Najafi F, Babaei E (2014): Dendrosomal curcumin nanoformulation downregulates pluripotency genes via miR-145 activation in U87MG glioblastoma cells. *Int J Nanomedicine* 9, 403–417
- Theppawong A, Van de Walle T, Grootaert C, Van Hecke K, Catry N, Desmet T, Van Camp J, D'hooghe M (2019): Synthesis of Non-Symmetrical Nitrogen-Containing Curcuminoids in the Pursuit of New Anticancer Candidates. *ChemistryOpen* 8, 236–247
- Unnikrishnan A, Gafken PR, Tsukiyama T (2010): Dynamic changes in histone acetylation regulate origins of DNA replication. *Nat Struct Mol Biol* 17, 430–437
- van Veldhuijzen Zanten SEM, Baugh J, Chaney B, Jongh D de, Sanchez Aliaga E, Barkhof F, Noltes J, Wolf R de, van Dijk J, Cannarozzo A et al. (2017): Development of the SIOPE DIPG network, registry and imaging repository: a collaborative effort to optimize research into a rare and lethal disease. *J Neurooncol* 132, 255–266
- Volak LP, Hanley MJ, Masse G, Hazarika S, Harmatz JS, Badmaev V, MAJEED M, Greenblatt DJ, Court MH (2013): Effect of a herbal extract containing curcumin and piperine on midazolam, flurbiprofen and paracetamol (acetaminophen) pharmacokinetics in healthy volunteers. *Br J Clin Pharmacol* 75, 450–462
- Wang D, Ge S, Bai J, Song Y (2018): Boswellic acid exerts potent anticancer effects in HCT-116 human colon cancer cells mediated via induction of apoptosis, cell cycle arrest, cell migration inhibition and inhibition of PI3K/AKT signalling pathway. *J BUON* 23, 340–345
- Wang L, Ye X, Cai X, Su J, Ma R, Yin X, Zhou X, Li H, Wang Z (2015): Curcumin suppresses cell growth and invasion and induces apoptosis by down-regulation of Skp2 pathway in glioma cells. *Oncotarget* 6, 18027–18037
- Wang Y, Ying X, Xu H, Yan H, Li X, Tang H (2017): The functional curcumin liposomes induce apoptosis in C6 glioblastoma cells and C6 glioblastoma stem cells in vitro and in animals. *Int J Nanomedicine* 12, 1369–1384
- Ward E, DeSantis C, Robbins A, Kohler B, Jemal A (2014): Childhood and adolescent cancer statistics, 2014. *CA Cancer J Clin* 64, 83–103
- Wiese M, Hamdan FH, Kubiak K, Diederichs C, Gielen GH, Nussbaumer G, Carcaboso AM, Hulleman E, Johnsen SA, Kramm CM (2020): Combined treatment with CBP and BET inhibitors reverses inadvertent activation of detrimental super enhancer programs in DIPG cells. *Cell Death Dis* 11, 673
- Wu GQ, Chai KQ, Zhu XM, Jiang H, Wang X, Xue Q, Zheng AH, Zhou HY, Chen Y, Chen XC et al. (2016): Anti-cancer effects of curcumin on lung cancer through the inhibition of EZH2 and NOTCH1. *Oncotarget* 7, 26535–26550
- Xi Y, Gao H, Callaghan MU, Fribley AM, Garshott DM, Xu ZX, Zeng Q, Li YL (2015): Induction of BCL2-Interacting Killer, BIK, is Mediated for Anti-Cancer Activity of Curcumin in Human Head and Neck Squamous Cell Carcinoma Cells. *J Cancer* 6, 327–332

- Xu C, Liu X, Geng Y, Bai Q, Pan C, Sun Y, Chen X, Yu H, Wu Y, Zhang P et al. (2017): Patient-derived DIPG cells preserve stem-like characteristics and generate orthotopic tumors. *Oncotarget* **8**, 76644–76655
- Xu XY, Meng X, Li S, Gan RY, Li Y, Li HB (2018): Bioactivity, Health Benefits, and Related Molecular Mechanisms of Curcumin: Current Progress, Challenges, and Perspectives. *Nutrients* **10**, 1553
- Yan X, Pan B, Lv T, Liu L, Zhu J, Shen W, Huang X, Tian J (2017): Inhibition of histone acetylation by curcumin reduces alcohol-induced fetal cardiac apoptosis. *J Biomed Sci* **24**, 1
- Yeh WL, Lin HY, Huang CY, Huang BR, Lin C, Lu DY, Wei KC (2015): Migration-prone glioma cells show curcumin resistance associated with enhanced expression of miR-21 and invasion/anti-apoptosis-related proteins. *Oncotarget* **6**, 37770–37781
- Yin H, Zhou Y, Wen C, Zhou C, Zhang W, Hu X, Wang L, You C, Shao J (2014): Curcumin sensitizes glioblastoma to temozolomide by simultaneously generating ROS and disrupting AKT/mTOR signaling. *Oncol Rep* **32**, 1610–1616
- Yoshida K, Toden S, Ravindranathan P, Han H, Goel A (2017): Curcumin sensitizes pancreatic cancer cells to gemcitabine by attenuating PRC2 subunit EZH2, and the lncRNA PVT1 expression. *Carcinogenesis* **38**, 1036–1046
- Zanotto-Filho A, Braganhol E, Klafke K, Figueiró F, Terra SR, Paludo FJ, Morrone M, Brito IJ, Battastini AM, Forcelini CM et al. (2015): Autophagy inhibition improves the efficacy of curcumin/temozolomide combination therapy in glioblastomas. *Cancer Lett* **358**, 220–231
- Zarghooni M, Bartels U, Lee E, Buczkowicz P, Morrison A, Huang A, Bouffet E, Hawkins C (2010): Whole-genome profiling of pediatric diffuse intrinsic pontine gliomas highlights platelet-derived growth factor receptor alpha and poly (ADP-ribose) polymerase as potential therapeutic targets. *J Clin Oncol* **28**, 1337–1344
- Zhang C, Gao S, Molascon AJ, Liu Y, Andrews PC (2014): Quantitative Proteomics Reveals Histone Modifications in Crosstalk with H3 Lysine 27 Methylation. *Mol Cell Proteomics* **13**, 749–759
- Zhang T, Cooper S, Brockdorff N (2015): The interplay of histone modifications – writers that read. *EMBO Rep* **16**, 1467–1481
- Zhongfa L, Chiu M, Wang J, Chen W, Yen W, Fan-Havard P, Yee LD, Chan KK (2012): Enhancement of curcumin oral absorption and pharmacokinetics of curcuminoids and curcumin metabolites in mice. *Cancer Chemother Pharmacol* **69**, 679–689

Danksagung

Ich möchte mich herzlich bei meiner Betreuerin Frau Dr. Maria Wiese bedanken. Vielen Dank für die Unterstützung während meiner Dissertation, die vielen ermutigenden Worte, wenn ich sie brauchte und die hilfreiche und konstruktive Kritik. Danke auch für deine Erreichbarkeit und deine immer offenstehende Bürotür.

Weiterhin möchte ich mich bei Herrn Prof. Christof Kramm für die Möglichkeit, meine Dissertation in der Abteilung für pädiatrische Hämatologie und Onkologie durchführen zu können, bedanken. Vielen Dank für die gute Beratung und Unterstützung.

Zudem geht mein Dank an das Transcriptome and Genome Analysis Laboratory in Göttingen. Vielen Dank für die Unterstützung meines Projekts.

Ein besonderer Dank geht auch an Frau Anke Herbst und meine Laborkolleg*innen Klaudia, Therese, Eshana und Lennart. Danke, dass ihr meine Laborzeit durch Rat und Tat unterstützt habt.